Journal of South American Earth Sciences 122 (2023) 104099

Contents lists available at ScienceDirect

Journal of South American Earth Sciences

journal homepage: www.elsevier.com/locate/jsames

Isotopic constraints on Davis bank, Vitória-Trindade Ridge: A Revised Petrogenetic Model

Gabriella de Oliveira Amaral Quaresma [a], Anderson Costa dos Santos [a,*], Eduardo Reis Viana Rocha-Júnior [b], Juliana Bonifácio [a], Caio Assumpção Queiroz Rego [a], João Mata [c], Claudio de Morisson Valeriano [d], Fred Jourdan [e], Nadine Mattielli [f], Mauro César Geraldes [a]

[a] *Universidade do Estado do Rio de Janeiro (UERJ), Faculdade de Geologia, Departamento de Mineralogia e Petrologia Ígnea, Rua São Francisco Xavier, 524 - 4° Andar/bloco A, Rio de Janeiro (RJ), Brazil*

[b] *Universidade Federal da Bahia (UFBA), Instituto de Física, Departamento de Física da Terra e do Meio Ambiente, Rua Barão de Jeremoabo, s/n, 40170-115, Salvador (BA), Brazil*

[c] *Instituto Dom Luiz, Faculdade de Ciências, Universidade de Lisboa, 1749-016, Lisboa, Portugal*

[d] *Laboratório de Geocronologia e Isótopos Radiogênicos (LAGIR), Faculdade de Geologia, Universidade do Estado do Rio de Janeiro (UERJ), Rua São Francisco Xavier, 524 - Maracanã, 20943-000, Rio de Janeiro (RJ), Brazil*

[e] *Western Australian Argon Isotope Facility, School of Earth, and Planetary Sciences, JdL Centre and TIGeR, Curtin University of Technology – GPO Box U1987, Perth, WA6845, Australia*

[f] *Université Libre de Bruxelles, Laboratoire G-Time, DGES, Av. Roosevelt, 50, CP, 160/02, 1050, Brussels, Belgium*

A R T I C L E I N F O

Keywords:
Sr-Nd-Pb Isotopic ratios
Mantle heterogeneity
Hybrid mantle
Brasiliano orogeny heritage
Vitória-trindade ridge (VTR)

A B S T R A C T

Davis Bank is the largest and most voluminous volcanic mount in the Vitória-Trindade Ridge (VTR), which comprehends a notable alignment of volcanic features on the South Atlantic Ocean, located at *ca.* 20°S. The VTR has been interpreted by some authors as the track of the Trindade hotspot impriented on the South American Plate, despite the evident importance of structural control on the ridge. This study presents the first integrated analysis of Sr-Nd-Pb isotopic compositions of Davis Bank to provide new constraints on its magmatic processess. We also present a new whole-rock ^{40}Ar/^{39}Ar *mini-plateau* age of 21.42 ± 0.13 Ma (P = 0.49) for one dredged sample from Davis Bank and new geochemical data. The Sr-Nd-Pb isotopic signature of Davis Bank rocks, along with isotopic signatures observed on the Vitória Seamount, are more enriched than the other magmatic manifestations of the VTR. This precludes the derivation of Davis Bank via the exclusive melting of a depleted mantle source, requiring the involvement of one or several enriched components homogenized before eruption. We propose that one of these components is related to the recycled subducted oceanic crust and evolved in an environment with time-integrated low Sm/Nd and slightly high Rb/Sr, U/Pb, and Th/Pb ratios. The enriched component is probably represented by a HIMU-type pyroxenite (hybrid component). Our modeling of the isotopic data indicates that Davis Bank isotopic composition is achieved by a dominant asthenospheric component (DMM) hybridized by the addition of EMI (< 24% in the mixing) and HIMU (up to 20% in the mixture) melts. We further argue that a deep-mantle origin associated with the Trindade Plume hypothesis lacks convincing evidence such as robust geochronological data to attest to the age progression along the VTR. We believe that the Vitória-Trindade Ridge is the surface manifestation of upwelling flow attributed to anomalous fertile shallow sources within a depleted mantle matrix with ubiquitous heterogeneities. Important contributions of detached SCLM fragments and subducted slabs from the Brasiliano Orogeny contaminating the mantle underneath the South Atlantic Ocean are suggested. The presence of such materials in the convective mantle may account for the significant shallow seismic anomalies that have been observed beneath many intraplate volcanic regions in the South Atlantic.

* Corresponding author. Grupo Tektos e GeoAtlântico, Universidade do Estado do Rio de Janeiro/Geobiotec, Departamento de Geociências, Universidade de Aveiro, 3810-193, Aveiro, Portugal.

E-mail addresses: gabriella.oaq@gmail.com (G. de Oliveira Amaral Quaresma), andcostasantos@gmail.com (A. Costa dos Santos), eduardo.junior@ufba.br (E.R.V. Rocha-Júnior), julianafbonifacio@gmail.com (J. Bonifácio), aqrcaio@gmail.com (C.A. Queiroz Rego), jmata@fc.ul.pt (J. Mata), valeriano.claudio@gmail.com (C. de Morisson Valeriano), f.jourdan@exchange.curtin.edu.au (F. Jourdan), mauro.geraldes@gmail.com (M.C. Geraldes).

https://doi.org/10.1016/j.jsames.2022.104099
Received 5 July 2022; Received in revised form 27 October 2022; Accepted 4 November 2022
Available online 5 November 2022

1. Introduction

The South Atlantic Ocean is characterized by several intraplate volcanic buildings, some of which constitute lineaments as aseismic ridges, seamounts, and islands (*e.g.*, Walvis Ridge, Tristan da Cunha, and Gough islands, Vitória-Trindade Ridge (VTR), St. Helena Seamounts). These lineaments are often considered to be related to hotspot tracks (*e.g.*, Chaffey et al., 1989; Bongiolo et al., 2015; Pires and Bongiolo, 2016; Santos and Hackspacher, 2021; Monteiro et al., 2021; Santos et al., 2021).

Geochemical studies of Ocean Island Basalts (OIB) are an essential tool for assessing mantle heterogeneity (*e.g.*, Hofman, 2014) since it is assumed that OIBs undergo minimal or no crustal contamination, thus providing precise constraints on the nature of the mantle. Significant heterogeneity is manifested by OIBs that vary in composition (tholeiitic to alkaline) and xhibit considerable elemental and isotopic diversity. The study of the isotopic systems of OIBs provides essential means for recognizing the composition of their mantle sources. Several isotopically distinct mantle sources have been proposed to explain such OIB variations (*e.g.*, "DMM", "EMI", "EMII", "HIMU", "FOZO", "C"; Zindler and Hart, 1986; Hart, 1988; Stracke et al., 2005), which may also differ lithologically (Mallik and Dasgupta, 2012), as suggested by the correlation, on a global scale, of $^{206}Pb/^{204}Pb$ and $^{87}Sr/^{86}Sr$ with the major element compositions of OIBs with high and near primary MgO content (Jackson and Dasgupta, 2008).

OIBs are more enriched in incompatible trace elements than the primitive mantle (Sun and McDonough, 1989), yet their Sr and Nd isotopic compositions indicate a time-integrated depletion in the more incompatible elements. In order to explain the origin of such enrichment, several authors often invoke the recycling of subducted oceanic crust, with or without sediments, continental crust, and the recycling of ancient metasomatized oceanic or continental lithosphere as the cause of mantle heterogeneity (*e.g.*, Jackson and Dasgupta, 2008; Hofman, 2014). As an alternative, the metasomatized lithospheric mantle has been invoked as a source for alkaline magmas (Pilet et al. 2011). Also, the primary source for OIBs has been more commonly associated with melting of lithologically heterogeneous mantle sources, such as eclogite or pyroxenite mixtures with peridotite (*e.g.*, Sobolev et al., 2005; Mallik and Dasgupta, 2012).

The VTR corresponds to a remarkable alignment of alkaline volcanic buildings offshore Brazil with progressively apparent younger ages eastward, which has been interpreted as the track of the Trindade Plume (Thompson et al., 1998; Skolotnev et al., 2011; Bongiolo et al., 2015; Santos, 2016; Santos et al. 2018a,b; Skolotnev and Peive, 2017; Santos et al., 2021; Maia et al., 2021). Although many geochemical and some geochronological studies have been carried out so far on the main islands of this alignment (Trindade and Martin Vaz; *e.g.*, Halliday et al., 1992; Marques et al., 1999; Siebel et al., 2000; Bongiolo et al. 2015; Pires and Bongiolo, 2016; Pires et al., 2016; Santos et al. 2018a, 2018b, 2021), both the precise age progression rate along the VTR and an understanding of the nature of each of the magmatic episodes remain elusive, mainly due to the sparse data available for the seamounts (Skolotnev et al., 2011; Peyve and Skolotnev, 2014; Santos, 2016; Skolotnev and Peive, 2017; Jesus et al., 2019; Maia et al., 2021).

Davis Bank differ from other VTR volcanic edifices by being composed of basanitic and more evolved rocks (tephrites), crystallized from a fractionated liquid (SiO_2: from 40.9 to 47.6 wt.%; MgO: from 3.6 to 9.6 wt.%) with strong enrichment in light rare earth elements (LREE) and large-ion lithophile elements (LILE), contrasting to the ultrabasic to intermediate magmas from the other seamounts as the melanephelinites from Montague and Jaseur Seamounts (Santos, 2016; Peyve and Skolotnev, 2014), ankaramite from Colúmbia Seamount (Fodor and Hanan, 2000) and Dogaressa Bank (Skolotnev et al., 2011) and alkaline basalt from Vitória Seamount (Maia et al., 2021; SiO_2 *ca.* 37 wt.%; MgO *ca.* 10 wt.%) and the nephelinitic-phonolitic successions presented in the Trindade-Martin Vaz archipelago (SiO_2 *ca.* 36–57 wt.%; MgO *ca.* 10–15 wt.%) (Marques et al., 1999, 2016; Bongiolo et al., 2015; Pires and Bongiolo, 2016; Santos et al., 2021; 2018a, 2018b, 2021).

To provide further information on the alkaline magmatism of the Vitória-Trindade Ridge, we here present new geochronological and isotopic data of samples from the volcanic episode that led to the formation of one of the largest physiographic features of the VTR alignment, the Davis Bank. We report new $^{40}Ar/^{39}Ar$ age data, Sr-Nd-Pb isotopic compositions and geochemical compositions from Davis Bank in combination with literature data (Halliday et al., 1992, Marques et al., 1999, Fodor and Hanan, 2000; Siebel et al., 2000; Peyve and Skolotnev, 2014; Bongiolo et al., 2015; Skolotnev and Peive, 2017; Santos et al., 2018a; Jesus et al., 2019; Maia et al., 2021) to elaborate a petrogenetic model that explains the isotopic signature of the studied rocks, as well as to discuss the associated tectonic settings.

2. Geologic setting

The VTR is the most longest aseismic ridge in the Brazilian offshore territory, extending about 1,170 km from the Vitória seamount, south Abrolhos Magmatic Complex, to the Trindade-Martin Vaz Archipelago, where the oceanic lithosphere is *ca.* 90–100 Ma (Muller et al., 2008). It includes the Trindade Island and the Martin Vaz Archipelago and several seamounts and banks, the most expressive of which are, from west to east: Vitória Seamount, Champlain Seamount, Colúmbia Bank, Besnard Bank, Montague Seamount, Jaseur Seamount, Davis Bank, Dogaressa Bank and Colúmbia Seamount (Fig. 1).

Davis Bank is located at the central portion of the Vitória-Trindade Ridge (20°51′ S; 34°47′ W), and it is the largest volcanic edifice on this ridge (Motoki et al., 2012; Alberoni et al., 2020). This voluminous volcanic structure (*ca.* 14,000 km^3) was formed during the Miocene (Aquitanian; Santos, 2016 and this work) and stands on a lithosphere with an inferred thickness of *ca.* 100 km (Conrad and Lithgow-Bertelloni, 2006). According to Motoki et al. (2012) and Alberoni et al. (2020), Davis Bank corresponds to a conic volcanic building, 4 km high, with a circular base of 60 km diameter and a planar top of 35 km diameter, with a total area of 11,304 km^2, and a volume of *ca.* 14,000 km^3.

Many authors consider the VTR alignment as resulting from the South American plate movement above the Trindade hotspot (*e.g.,* Gibson et al., 1995; VanDecar et al., 1995). Nonetheless, the existence of a deep-seated Trindade Plume and its magnitude is still controversial. Several authors highlight the structural control on the formation and evolution of this ridge since it spatially fits the Vitória-Trindade Fracture Zone (Fig. 2; *e.g.*, Ferrari and Riccomini, 1999; Alves et al., 2006; Barão et al., 2020; Alves et al., 2022).

Most of the Trindade Plume suggestions rely on the apparent progression of radiometric ages displayed along the VTR, despite the sparse geochronological data published so far, especially concerning the submarine edifices. Magmatic episodes from west to east along the ridge range from Eocene to Pleistocene (Fig. 1): Jaseur 29.8 ± 6.6 Ma (U–Pb zircon dating; Skolotnev et al., 2011); Davis *ca.* 21 Ma; ($^{40}Ar/^{39}Ar$ dating; Santos, 2016; Skolotnev and Peive, 2017, see references for details and this work); and the Trindade-Martin Vaz archipelago ranging from 3.4 to 0.3 Ma ($^{40}Ar/^{39}Ar$ dating; Santos et al., 2021; Santos, 2016; Pires et al., 2016; Santos et al., 2018a; Santos et al., 2021; Monteiro et al., 2021).

3. Materials and methods

Rocks were recovered by dredging using the research vessel Professor Logachev during a sampling study ungergone by the Brazilian Navy in 2010 as part of the Project "Deep Sea Dredging, Offshore Brazil" supported by FEMAR. Three samples (Table 1) were analyzed for Sr, Nd and Pb isotopes after 6M HCl acid leaching to eliminate the weakly bonded Sr resulting from alteration processes as detailed in next section.

The three samples analyzed were collected at the same site and are, in fact, fragments of the same rock. Therefore even though Pb isotope were analyzed in a different fragment (VIT-TRIN-DR-4G), it represents the same rock and, therefore, geochemistry matches those from samples VIT-TRIN-DR-4M; VIT-TRIN-DR-4N, as it is presented as a new geochemical data in Supplementary Table 2.

3.1. Sr–Nd isotopes

Two samples (VIT-TRIN-DR-4M; VIT-TRIN-DR-4N) were analyzed for Sr–Nd isotopes at the Laboratório de Geocronologia e Isótopos Radiogênicos (LAGIR) at the Universidade do Estado do Rio de Janeiro (UERJ). Analyses were performed using Thermo Scientific Triton Multicollector Thermal Ionization Mass Spectrometer (TIMS) (see Valeriano et al., 2003, for details on measurement procedures). Samples were dissolved, and Sr and Nd were separated following methods described in Heilbron et al. (2013). The isotopic ratios were normalized to $^{146}Nd/^{144}Nd = 0.7219$; $^{147}Sm/^{152}Sm = 0.5608$ and $^{88}Sr/^{86}Sr = 8.3752$. Repeated analyses on SRM-987 and JNdi-1 (Tanaka et al., 2000) standard reference materials yielded mean $^{87}Sr/^{86}Sr$ ratios of 0.710239 ± 0.000007 (2σ) and $^{143}Nd/^{144}Nd = 0.512100 \pm 0.000006$ (2σ). Analytical total procedure blanks during this study were less than 200 pg for Nd and less than 70 pg for Sm. Sr value for blank was not obtained.

3.2. Pb isotopes

Lead isotopic analyses for one sample (VIT-TRIN-DR-4G) were performed at the Laboratoire G-Time of the Université Libre de Bruxelles (ULB, Belgium) on a Nu Plasma I Multi-Collector Inductively Coupled Plasma Mass Spectrometer (MC-ICP-MS). Pb isotopic compositions were measured by Tl addition with Pb–Tl concentration ratio of ± 5:1 (for a minimum signal of 100 mV in the axial collector - ^{204}Pb). ^{202}Hg was routinely monitored to correct for the potential isobaric interference of ^{204}Hg on ^{204}Pb. Mass discrimination was monitored using ln-ln plots and corrected by the external normalization and the standard sample bracketing technique using the recommended values of Galer and Abouchami (1998 - *i.e.,* $^{206}Pb/^{204}Pb = 16.9405 \pm 15$; $^{207}Pb/^{204}Pb = 15.4963 \pm 16$; $^{208}Pb/^{204}Pb = 36.7219 \pm 44$). The repeated measurements of the NBS981 gave the following values: $^{206}Pb/^{204}Pb = 16.9403 \pm 8$, $^{207}Pb/^{204}Pb = 15.4961 \pm 10$, $^{208}Pb/^{204}Pb = 36.7217 \pm 31$ (2σ) for the NBS981 Pb standard (5 runs).

3.3. $^{40}Ar/^{39}Ar$ geochronology

$^{40}Ar/^{39}Ar$ dating procedures were performed at the Western Australian Argon Isotope Facility at Curting University, Perth, Australia. We selected one fresh sample (VIT-TRIN-DR-4M) from Davis Seamount for $^{40}Ar/^{39}Ar$ dating and separated unaltered, 200-300 μm-size, groundmass particles from where we removed as much phenocrysts as

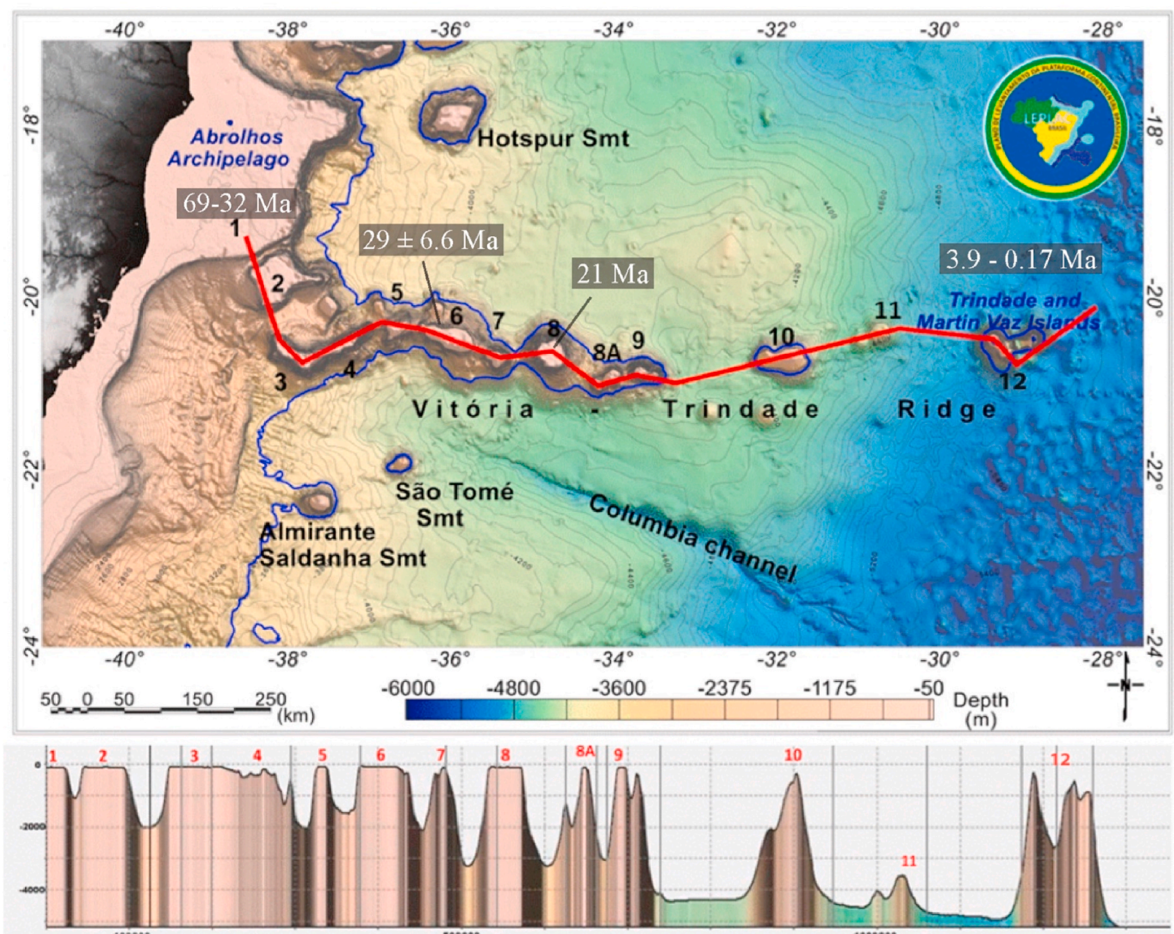

Fig. 1. - Color DTM showing the main physiographies associated with the VTR. From West to East: (1) Abrolhos Volcanic Complex (ages from Cordani, 1970; Fodor et al., 1983; Mohriak, 2005); (2) Besnard Bank; (3) Vitória Seamount; (4) Congress Bank; (5) Montague Seamount; (6) Jaseur Seamount (age from Skolotnev et al., 2011); (7) Colúmbia Bank; (8) Davis Bank (ages from Santos, 2016; Skolotnev and Peive, 2017); (8A); Asmus Bank; (9) Dogaressa Bank; (10) Colúmbia Seamount; (11) Palma Seamount and (12) Trindade and Martin Vaz Islands (ages from Cordani, 1970; Pires et al., 2016; Santos et al., 2021; 2021; Santos and Hackspacher, 2021; Santos et al., 2022a,b,c). The blue line depicts the 3500 m isobath and highlights the morphology continuity of the easternmost portion of the VTR.

possible to ensure a minimum level of excess $^{40}Ar^{*}$, if present (Sharp and Renne, 2005). These grains were separated using a Frantz magnetic separator and then carefully hand-picked under a binocular microscope. The selected groundmass grains were further leached in diluted HF for 1 min and then thoroughly rinsed with distilled water in an ultrasonic cleaner. Samples were loaded into six large wells of 1.9 cm diameter and 0.3 cm depth aluminum disc. These wells were bracketed by small wells that included Fish Canyon sanidine (FCs) used as a neutron monitor for which an age of 28.294 ± 0.036 Ma (1σ) was adopted (Renne et al.,

Table 1
Location of the samples dredged during the project “Deep Sea Dredging, offshore Brazil".

Samples	Latitude	Longitude	Depth (m)	Lithology
VIT-TRIN-DR-4G; VIT-TRIN-DR-4M; VIT-TRIN-DR-4N;	20°51′38.40″ S	34°47′52.20″ W	– 1,940 m	Basanite

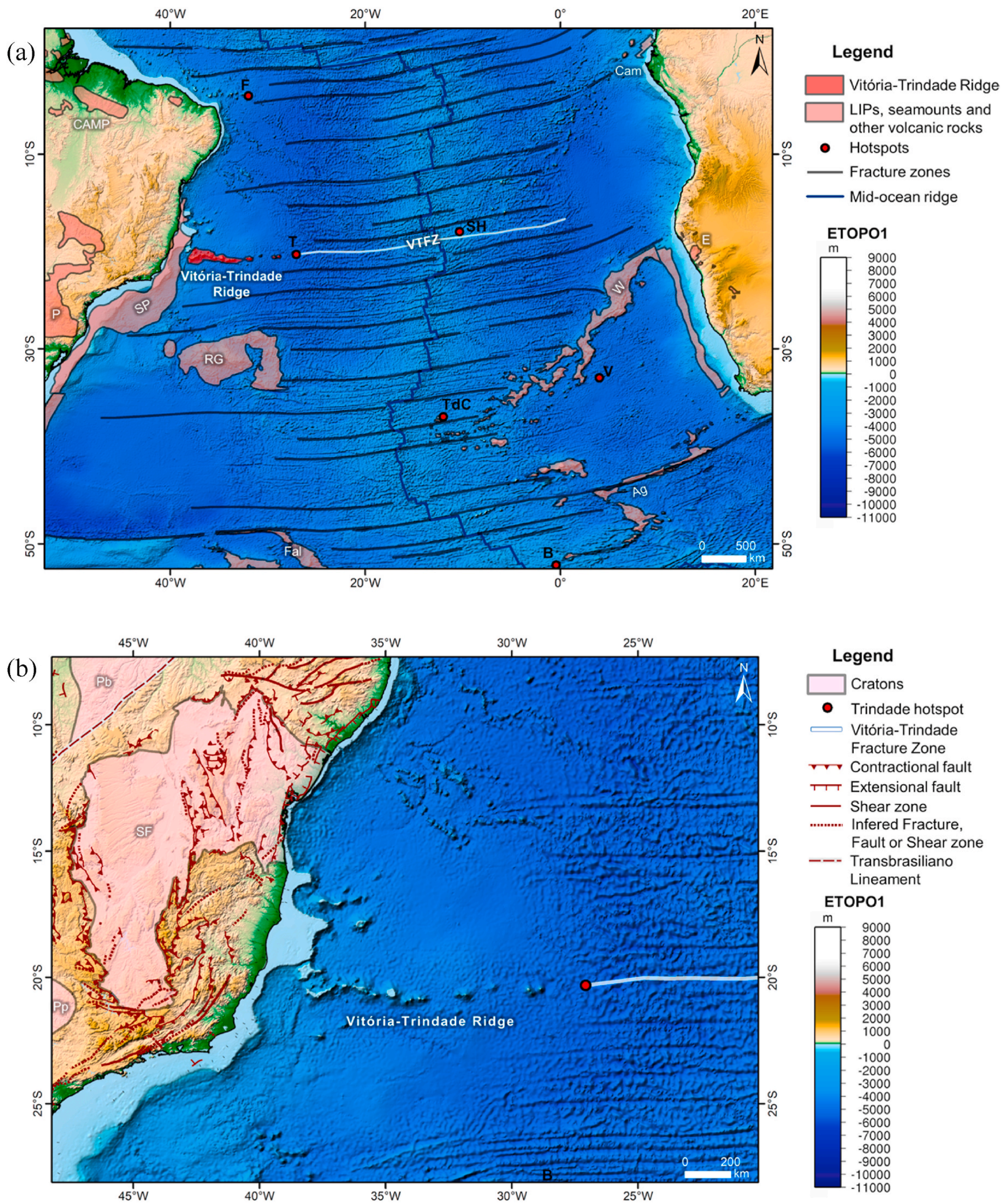

Fig. 2. – (a) Map of the South Atlantic Ocean, with topography and bathymetry from ETOPO1 Global Relief Model (NOAA). LIPs, seamounts, volcanic rocks (Ag.: Agulhas Ridge; Cam.: Cameroon; CAMP: Central Atlantic Magmatic Province; E: Etendeka; Fal.: Falkland; P: Paraná; RG.: Rio Grande Rise; SP.: São Paulo Plateau; W.: Walvis Ridge), hotspots (B.: Bouvet; F.: Fernando; SH.: St. Helena; T.: Trindade; TdC.: Tristan da Cunha; V.: Vema), fracture zones (VTFZ: Vitória Trindade Fracture Zone) and the mid-ocean ridge are shown. (b) Map of the South-East Brazilian Passive Margin depicting the onshore structures from Cordani et al. (2016).

2011). The discs were Cd-shielded (to minimize undesirable nuclear interference reactions) and irradiated for 2 h in the Hamilton McMaster University nuclear reactor (Canada) in position 5C. The mean J-values computed from standard grains within the small pits range from 0.00069840 ± 0.00000175 (0.25%) to 0.00069610 ± 0.00000299 (0.43%), determined as the average and standard deviation of J-values of the small wells for each irradiation disc. Mass discrimination was monitored using an automated air pipette and provided a mean value of 1.005376 ± 0.34 (% 1σ) per Dalton (atomic mass unit) relative to an air ratio of 298.56 ± 0.31 (Lee et al., 2006). The correction factors for interfering isotopes were ($^{39}Ar/^{37}Ar$) Ca = 7.30 × 10–4 (± 11%), ($^{36}Ar/^{37}Ar$) Ca = 2.82 × 10–4 (± 1%) and ($^{40}Ar/^{39}Ar$) K = 6.76 × 10–4 (± 32%).

The sample was step-heated in a double vacuum high-frequency Pond Engineering© furnace. The gas was purified in a stainless-steel extraction line using two AP10 and one GP50 SAES getters and a liquid nitrogen condensation trap. Ar isotopes were measured in static mode using a MAP 215-50 mass spectrometer (resolution of *ca.* 400; sensitivity of 4 × 10^{-14} mol/V) with a Balzers SEV 217 electron multiplier mainly using 9 to 10 cycles of peak-hopping. The data acquisition was performed with the Argus program written by M.O. McWilliams and ran under a LabView environment. The raw data were processed using the ArArCALC software (Koppers, 2002) and the ages were calculated using the decay constants recommended by Renne et al. (2010). Blanks were monitored every 3 to 4 steps and typical ^{40}Ar blanks range from 1 × 10^{-16} to 2 × 10^{-16} mol. Ar isotopic data corrected for blank, mass discrimination and radioactive decay are given in Supplementary Table 1 at the 1σ level. Our criteria for the determination of plateau are as follows: (i) plateaus must include at least 70% of ^{39}Ar; (ii) the plateau should be distributed over a minimum of three consecutive steps (iii) agreeing at 95% confidence level and satisfying a probability of fit (P) of at least 0.05. Plateau ages (Supp. Table 1 and Fig. 7) are given at the 2σ level and are calculated using the mean of the entire plateau steps, each weighted by the inverse variance of their individual analytical error. Mini plateaus are defined similarly, except that they include between 50% and 70% of ^{39}Ar and are considered less reliable than their plateau counterparts. Inverse isochrons include the maximum number of steps with a probability of fit ≥0.05. All sources of uncertainties are included in the calculation.

3.4. Mixing methodology

Modeling mixing calculations were performed using methods as in Rocha Júnior et al. (2013), Marques et al. (2018), Rocha-Junior et al. (2020) and Maia et al. (2022, in press). For the calculations, a two-step binary mixing with three compontents was used based on the mixing equation from DePaolo and Wasserburg (1979; and references therein). Firstly, a mixing process between the DMM and EMI components was modeled, in wich the hybrid composition was extracted and the result of the calculated composition was modeled with the third component (HIMU). We recalculate the outcome to a 100% base. We emphasize that a two-step mixing calculation has no significant mathematical difference than a ternary mixing calculation.

4. Results

4.1. Sr-Nd-Pb isotopes

The bulk rock Sr–Nd isotopic compositions of the Davis Bank and those of the Vitória seamount are distinct from that of the depleted mantle and differ from the other seamounts and islands from the VTR (Supplementary Table 1). The $^{87}Sr/^{86}Sr$ measured values of volcanic rocks of the Davis Bank range from 0.704014 to 0.704036, which are similar to the Vitória Seamount (0.704054 and 0.704031; Maia et al., 2021) and are at the higher end of the range defined by other VTR samples (0.703611–0.704130; Halliday et al., 1992; Marques et al., 1999; Fodor and Hanan, 2000; Siebel et al., 2000; Bongiolo et al., 2015; Skolotnev and Peive, 2017; Santos et al., 2018a). In addition, they have a more radiogenic composition than the Abrolhos Volcanic Complex (AVC; 0.703607–0.703946; Fodor et al., 1989). The Davis Bank rocks have a measured $^{143}Nd/^{144}Nd$ ranging from 0.512622 to 0.512636, or εNd ranging from - 0.3 to 0. The $^{143}Nd/^{144}Nd$ of Davis is similar to those of the Vitória Seamount (Maia et al., 2021) and less radiogenic than those previously reported for the other VTR volcanic edifices ($^{143}Nd/^{144}Nd$ = 0.51272–0.512879, ε_{Nd} = +3.0; Halliday et al., 1992; Marques et al., 1999; Fodor and Hanan, 2000; Siebel et al., 2000; Bongiolo et al., 2015; Skolotnev and Peive, 2017; Santos et al., 2018a).

In the $^{87}Sr/^{86}Sr$ *versus* $^{143}Nd/^{144}Nd$ space (Fig. 3), Davis Bank samples deviate significantly from the compositions of the depleted mantle (DMM) and other VTR samples (including Trindade and Martin Vaz islands), plotting within the EM1 field and overlaping the Sr–Nd isotope compositions of the Vitória Seamount (Maia et al., 2021).

Lead isotopic analysis yielded moderately radiogenic ratios of $^{206}Pb/^{204}Pb$ = 19.146, $^{207}Pb/^{204}Pb$ = 15.585 and $^{208}Pb/^{204}Pb$ = 39.321. The $^{207}Pb/^{204}Pb$ *versus* $^{206}Pb/^{204}Pb$ and $^{208}Pb/^{204}Pb$ *versus* $^{206}Pb/^{204}Pb$ diagrams (Fig. 4) show the isotopic compositions of the analyzed samples plotted together, for comparison, with the previously published data from VTR and the fields for South Atlantic plume-related rocks. On Pb isotope correlation diagrams, Davis Bank Pb isotopic signature matches most data from VTR (Halliday et al., 1992; Siebel et al., 2000; Fodor and Hanan, 2000; Peyve and Skolotnev, 2014), and all samples plot above the Northern Hemisphere Reference Line (NHRL, Hart, 1988), with Δ7/4 = 1.1 and Δ8/4 = 57.5 for Davis Bank lead values. The $^{206}Pb/^{204}Pb$ ratio correlates positively with $^{208}Pb/^{204}Pb$ ratios (r^2 = 0.84) and less significantly with $^{207}Pb/^{204}Pb$ (r^2 = 0.34) even when an offset sample from Colúmbia seamount is discarded. Davis Bank isotopic compositions together with compiled data from VTR are presented in Supplementary Table 1. We also present a compilation of whole-rock compositions previously published of Davis Bank and other VTR seamounts and banks (Supplementary Table 2).

4.2. $^{40}Ar/^{39}Ar$ ages

Analytical results of a basanite sample (2.94 wt% K_2O; LOI = 1.98%; see Jesus et al., 2019 for details) from Davis Bank are presented below. The step heating technique for $^{40}Ar/^{39}Ar$ whole rock dating was used. One of the conditions for obtaining a *plateau* age is that at least 70% of the gas released by the grain has approximate ages. In the diagram (Fig. 5), the age spectrum shows a relatively flat region between 1,100 °C and 1,300 °C, corresponding to 53.53% of the released gas, which we interpreted as a mini-*plateau* and yielded a weighted mean age of 21.42 ± 0.13 Ma (MSWD = 0.9; P = 43%). Although mini plateaus indicate that the system has been substantially perturbed, being less reliable than full plateau, we consider this weighted mean age to represent the best estimate for the eruption age of this sample (see discussion in 5.1).

5. Discussion

5.1. Age of the Davis Bank

The $^{40}Ar/^{39}Ar$ whole-rock age reported herein (21.42 ± 0.13 Ma) is consistent with ages previously published for Davis Bank, suggesting that it represents the eruption age. Indeed, Santos (2016) reported a remarkably similar age for a Davis Bank tephrite sample (21.57 ± 0.10 Ma; $^{40}Ar/^{39}Ar$ whole rock dating) and Skolotnev and Peive (2017), using the $^{40}Ar/^{39}Ar$ method on plagioclase and clinopyroxene yielding ages of 19.2 ± 0.7 Ma and 21.1 ± 1.6 Ma, respectively.

The Ar–Ar geochronological is supported by paleontological data. Indeed, Skolotnev et al. (2011), based on examination of the species composition of foraminifera and nannoplankton populations, have established an age for the carbonate platforms at the top of Davis and

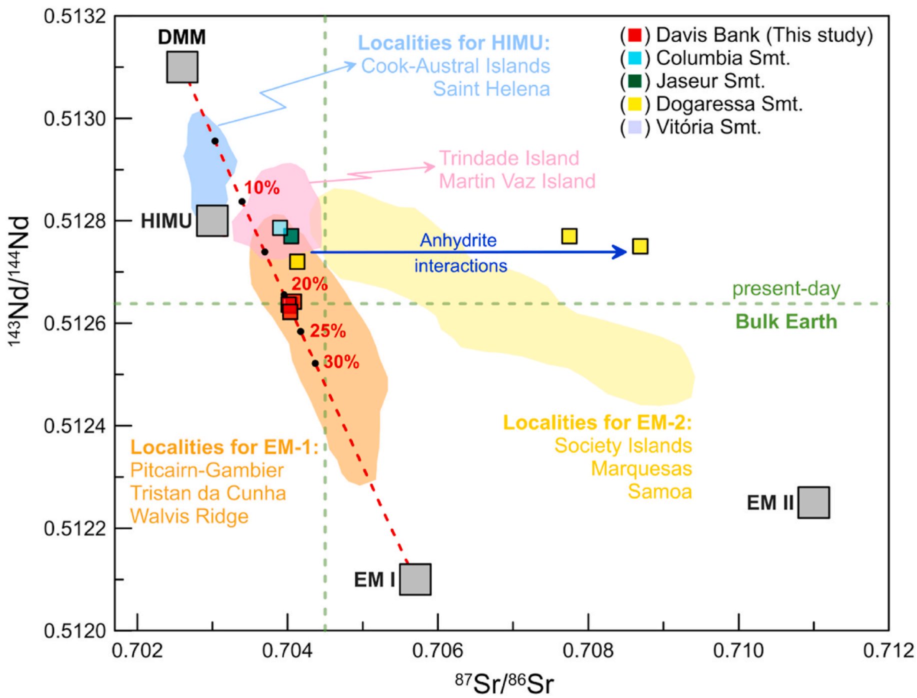

Fig. 3. - Plot of two-step binary mixing calculations (dashed lines) between DMM, EMI and HIMU-type pyroxenite to describe $^{87}Sr/^{86}Sr$ and $^{143}Nd/^{144}Nd$ isotopic variability of Davis bank and other VTR rocks. Modeling assumes two-component mixing between asthenospheric mantle represented by DMM - ($^{87}Sr/^{86}Sr = 0.7026$, [Sr] = 160 ppm, $^{143}Nd/^{144}Nd = 0.5131$, [Nd] = 9.6 ppm), EMI - ($^{87}Sr/^{86}Sr = 0.7057$, [Sr] = 495 ppm, $^{143}Nd/^{144}Nd = 0.5121$, [Nd] = 30.6 ppm). The parameters for the DMM, EMI, EMII and HIMU are from Zindler and Hart (1986), Salters and Stracke (2004), Workman and Hart (2005), Jackson and Dasgupta (2008), Gurenko et al. (2009), Hofman (2014) and Marques et al. (2018). The Sr and Nd contents of the EMI and HIMU endmembers are based on data from the GEOROC database (http://georoc.mpch-mainz.gwdg.de/georoc/), whereas for the melt DMM, the Sr and Nd contents were calculated considering a partial melting degree of *ca.* 3% (based on the study by Maia et al., 2021; bulk $D_{Sr} = 0.0185$ and $D_{Nd} = 0.0317$). Red dotted lines represents the mixing curves with the percenteges of contribution of the EMI component in a binary mixing with DMM depicted in red. Discussions on mixing calculations will be presented in section 5.

Dogaressa banks of *ca.* 19–24 Ma, pointing that the formation of the carbonates was close to the end of the volcanic activity in these paleo volcanoes (see Skolotnev et al., 2011 for further details).

According to Skolotnev and Peive (2017), the ages determined by absolute geochronology for Davis Bank samples (*ca.* 21 Ma) should represent the time of the last volcanic events on the bank due to the similarity with the ages of the superimposed limestones and the fact that the volcanic samples were collected at the upper portions of the bank slopes. These authors, assuming a fixed hotspot hypothesis and calculating the time of the volcanic onset from the half-spreading rate (about 2 cm/yr), suggested that volcanic activity in Davis Bank may have begun about 31 Ma, which indicates a long-term (*ca.* 10 Ma) building up for this volcanic building, spanning into the time from the Late Oligocene to Early Miocene (Skolotnev and Peive, 2017; and references therein).

5.2. *On the heterogeneity of the VTR magmatism*

As outlined before, Davis Bank is not only the most voluminous volcanic building of the VTR, but also displays several characteristics distinct from the other seamounts and the Trindade-Martin Vaz archipelago. Isotopic analyses here presented for the Davis Bank, alongside whole-rock data and mineral chemistry (Jesus et al., 2019), confirm those suggestions. For instance, according to Jesus et al. (2019), Davis Bank lavas show enrichment in incompatible elements (La/Sm_N *ca.* 4.1 and La/Yb_N *ca.* 21.7) when compared with the alkaline rocks from other seamounts (La/Sm_N = *ca.* 2.57; La/Yb_N = *ca.* 20 – compiled data from Maia et al., 2021). They are also characterized by lower contents of MgO (4.0 wt.%) and higher SiO_2 contents (*ca.* 45 wt.%), which differs from the ultrabasic seamounts (*ca.* 37 wt.% SiO_2; *ca.* 10 wt.% MgO) like the ankaramite from Colúmbia Seamount (Fodor and Hanan, 2000) and Dogaressa Bank (Skolotnev et al., 2011), melanephelinites from Montague and Jaseur Seamounts (Santos, 2016) and alkaline basalt from Vitória Seamount (Maia et al., 2021). Isotope ratios of Davis Bank are different from the majority of other occurrences of VTR, except for Vitória seamount (see below). Therefore, the variations mentioned above on the enrichment of incompatible elements cannot be assigned solely to differences in the extent of partial melting or to the distinct degrees of magmatic evolution.

Davis Bank is formed by ultrabasic to basic volcanic rocks, such as picro-basalt, olivine basalts, basanites and tephrites (Skolotnev et al., 2011; Peyve and Skolotnev, 2014; Jesus et al., 2019; Santos, 2016). These rocks range from aphiric to porphyritic and micro-glomeroporphyritic, with phenocrysts of olivine, clinopyroxene and plagioclase (Peyve and Skolotnev, 2014; Jesus et al., 2019; Santos, 2016). The rocks matrix are formed by some apatite, oxides, clinopyroxene and olivine, and some have a large amount of plagioclase and k-feldspar microlites (Peyve and Skolotnev, 2014; Jesus et al., 2019; Santos, 2016). According to Skolotnev et al. (2011) the more porphyritic rocks and those with olivine phenocrysts have the highest MgO (7–15.78 wt.%) and CaO (*ca.* 11 wt.%) contents and the lowest silica content (*ca.* 40–41 wt.%), in relation to the aphiric and less porphyritic rocks which, in turn, have higher Na_2O content (*ca.* 4 wt.%) (SiO_2 *ca.* 45 wt.%; MgO *ca.* 4 wt.%; CaO *ca.* 8 wt.%; Peyve and Skolotnev, 2014). The three samples from this study are less porphyritic rocks containing millimetric sparse phenocrysts of plagioclase as the most abundant phase, clinopyroxene and opaques. Samples from this work also show greater enrichment in incompatible elements and REEs (Supplementary Table 2), being the most evolved when compared to other submarine buildings and islands.

Although some authors have previously reported a restricted range in the isotopic signature along the VTR (*e.g.*, Skolotnev and Peive, 2017), the dredged samples from the Davis Bank (this study) and Vitória Seamount (Maia et al., 2021) show more unradiogenic Nd isotopic compositions (εNd varies from − 0.3 to 0) than other VTR rocks (ε_{Nd} varies from + 2.3 to + 4.1) pointing to the heterogeneity of the mantle sources feeding the magmatism along the VTR. Our interpretation is at odds with the idea of the possible homogeneity of the VTR magma source as previously proposed by Peyve and Skolotnev (2014) and Bongiolo et al. (2015). However, amount of samples for VTR is still very poor and any conclusions about homogeneity or heterogeneity are premature, although the data obtained so far points to the existence of a slightly heterogeneous mantle source.

As shown in Fig. 3, two samples from the Dogaressa seamount are strongly radiogenic in Sr isotopes. We suggest that this increase in the Sr isotopic compositions of the Dogaressa seamount rocks can potentially be attributed to the interaction with seawater or to a limited extent of

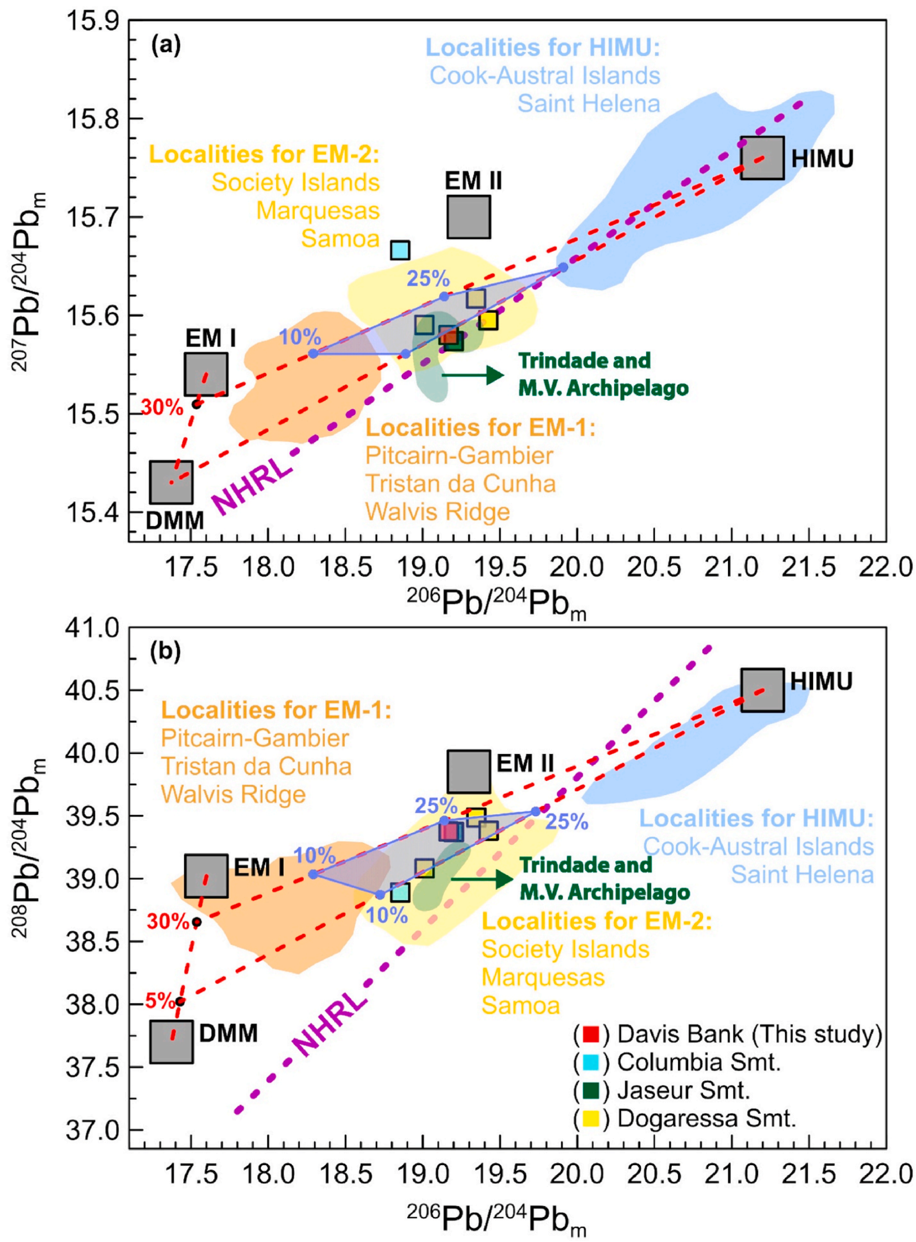

Fig. 4. - Plot of two-step binary mixing calculations (dashed lines) between DMM, EMI and HIMU-type pyroxenite to describe measured (m) $^{206}Pb/^{204}Pb$, $^{207}Pb/^{204}Pb$ and $^{208}Pb/^{204}Pb$ isotopic variability of Davis bank and other VTR rocks. Modeling assumes three-component mixing between asthenospheric mantle represented by DMM - ($^{206}Pb/^{204}Pb = 17.375$, $^{207}Pb/^{204}Pb = 15.430$, $^{208}Pb/^{204}Pb = 37.700$, [Pb] = 0.46 ppm), EMI - ($^{206}Pb/^{204}Pb = 17.600$, $^{207}Pb/^{204}Pb = 15.540$, $^{208}Pb/^{204}Pb = 39.020$, [Pb] = 2.82 ppm) and HIMU-type pyroxenite - ($^{206}Pb/^{204}Pb = 21.200$, $^{207}Pb/^{204}Pb = 15.760$, $^{208}Pb/^{204}Pb = 40.500$, [Pb] = 2.73 ppm). The parameters for the DMM, EMI, EMII and HIMU are from Zindler and Hart (1986), Salters and Stracke (2004), Workman and Hart (2005), Jackson and Dasgupta (2008), Gurenko et al. (2009), Hofman (2014) and Marques et al. (2018). The Pb content of the EMI and HIMU end-members are based on data from the GEOROC database (http://georoc.mpch-mainz.gwdg.de/georoc/), whereas for the melt DMM, the Pb content was calculated considering a partial melting degree of *ca.* 3% (based on the study by Maia et al., 2021; $D_{Pb} = 0.0092$). Red dotted lines represents the mixing curves with the percenteges of contribution of the EMI component in a first binary mixing with DMM depicted in red and the percenteges of contributions of the HIMU component in a second binary mixing between the hybrid component resulted form the first mixing depicted in purple. The mixing calculations indicate an EMI contribution in the depleted asthenospheric mantle (DMM) ranging from 5% to 30%.

assimilation of anhydrite-rich, evaporitic sediments, which may be found in the sedimentary sequence that underlies the oceanic basin (Fig. 3). Therefore, these high-radiogenic Sr samples will not be considered to assess mantle sources.

5.3. Identification and quantification of mantle source components involved in the Davis Bank magmatism

Overall, previously published VTR analyses plot in the $^{87}Sr/^{86}Sr$ and $^{143}Nd/^{144}Nd$ diagram between the compositions of DMM and present-day Bulk Earth (Fig. 3). However, the studied samples from Davis Bank (Skolotnev et al., 2011; Santos, 2016; Skolotnev and Peive, 2017 and this work) and Vitória Seamount (Maia et al., 2021) deviate from the DMM end-member by their more unradiogenic Nd, suggesting a more significant contribution of the EMI end-member. The moderately radiogenic $^{206}Pb/^{204}Pb$ composition from the Davis Bank sample reported herein cannot be explained by a mixing only involving DMM and EMI components. It may indicate a contribution of a HIMU mantle component, as suggested by Pires and Bongiolo (2016) for the Trindade Island, a hypothesis that we extend to all the other seamounts and islands of VTR. Therefore, we propose that a heterogeneous three-component mantle source (DMM, EMI, HIMU) in variable proportions could be envisaged to explain isotopic variability seen in VTR volcanic bodies. This is also shown in diagrams $^{206}Pb/^{204}Pb$ *versus* $^{143}Nd/^{144}Nd$ (Fig. 6), which reveal that a two-component mixing model does not explain the variations in the VTR. It suggests that the mantle source from which these rocks were derived possibly included a mixture between a HIMU-type component and depleted mantle material with a significant admixture of an EM-like component, which according to the positioning into the Sr–Nd isotopic space, must be of the EMI-type. All diagrams reinforce the similarities between isotopic signatures of Davis Bank and Vitória Seamount.

Model mixing calculations between DMM and EMI components for Nd and Sr isotopic compositions suggest that EMI contributions ranging from 5% to 30% can account for the observed Davis rocks compositions. As it is clear from isotope correlation diagrams of $^{206}Pb/^{204}Pb$ *versus* $^{143}Nd/^{144}Nd$, $^{207}Pb/^{204}Pb$ and $^{208}Pb/^{204}Pb$ isotope ratios, as well as $^{87}Sr/^{86}Sr$ *versus* $^{143}Nd/^{144}Nd$, only the DMM and EMI components

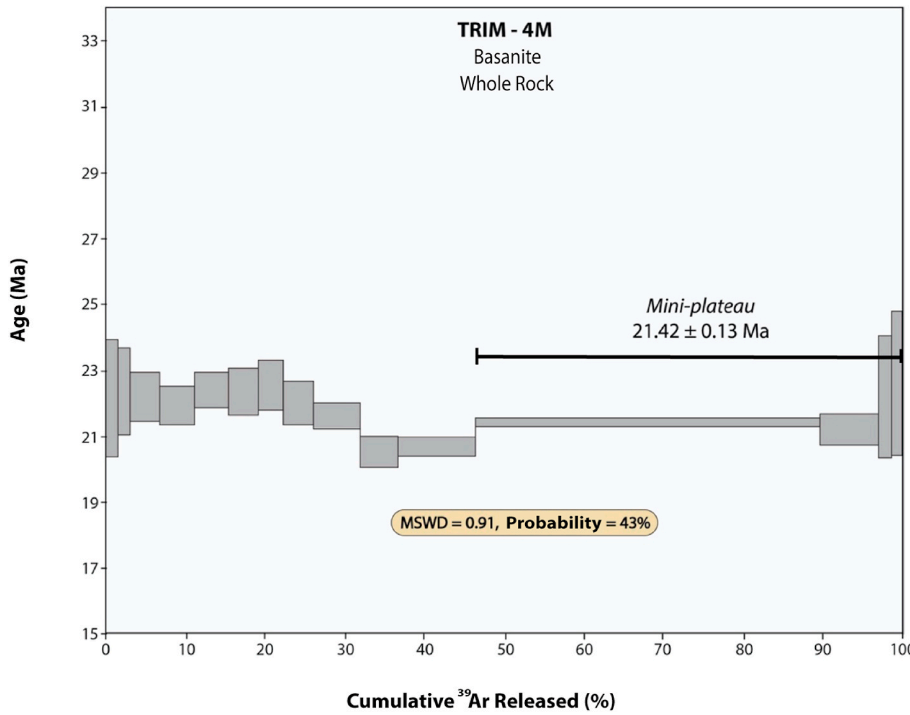

Fig. 5. - Plateau age diagram for sample TRIM-04M (basanite; 1.25% K_2O; LOI 1.98%) – Davis Bank.

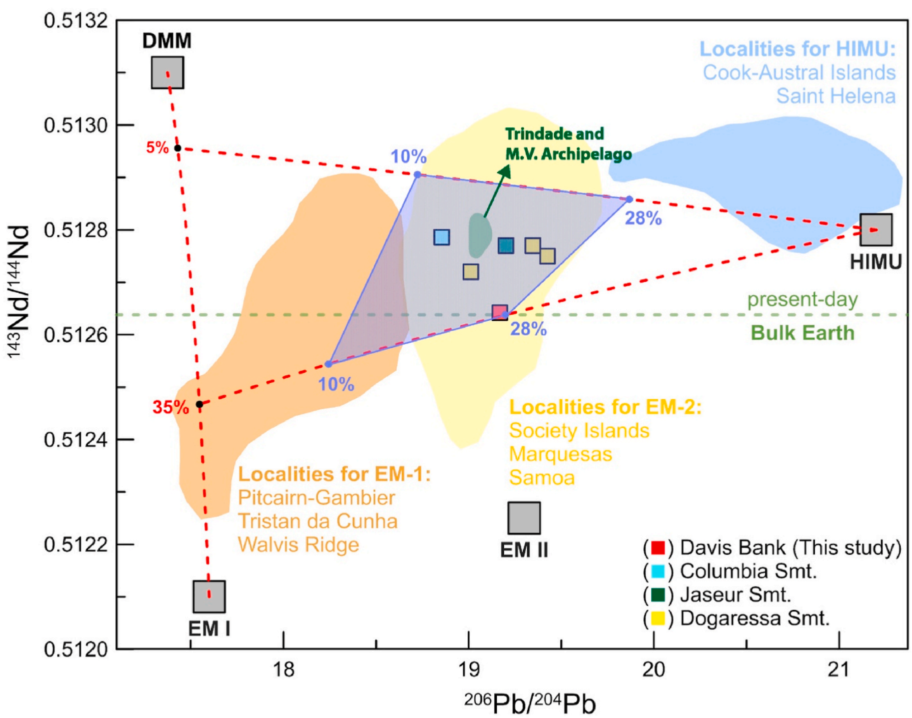

Fig. 6. - Plot of two-step binary mixing calculations (dashed lines) between DMM, EMI and HIMU-type pyroxenite to describe $^{143}Nd/^{144}Nd$ and $^{206}Pb/^{204}Pb$ isotopic variability of Davis bank and other VTR rocks. Modeling assumes three-component mixing between asthenospheric mantle represented by DMM – ($^{143}Nd/^{144}Nd$ = 0.5131, [Nd] = 9.6 ppm, $^{206}Pb/^{204}Pb$ = 17.375, [Pb] = 0.46 ppm), EMI - ($^{143}Nd/^{144}Nd$ = 0.5121, [Nd] = 30.6 ppm, $^{206}Pb/^{204}Pb$ = 17.600, [Pb] = 2.82 ppm) and HIMU-type pyroxenite - ($^{143}Nd/^{144}Nd$ = 0.5128; [Nd] = 45.7 ppm, $^{206}Pb/^{204}Pb$ = 21.200, [Pb] = 2.73 ppm). The parameters for the DMM, EMI, EMII and HIMU are from Zindler and Hart (1986), Salters and Stracke (2004), Workman and Hart (2005), Jackson and Dasgupta (2008), Gurenko et al. (2009), Hofman (2014) and Marques et al. (2018). The Sr and Nd contents of the EMI and HIMU endmembers are based on data from the GEOROC database (http://georoc.mpch-mainz.gwdg.de/georoc/), whereas for the melt DMM, the Sr and Nd contents were calculated considering a partial melting degree of *ca.* 3% (based on the study by Maia et al., 2021; bulk D_{Nd} = 0.0317 and D_{Pb} = 0.0092).

cannot explain the isotopic variations in VTR lavas, requiring a third component that can explain the more radiogenic $^{206}Pb/^{204}Pb$, $^{207}Pb/^{204}Pb$ and $^{208}Pb/^{204}Pb$ isotopic ratios. The best fit in terms of Nd, Pb, and Sr isotopic compositions is attained through the partial melting of a DMM-type depleted source mixed with EMI (< 24% in the mixing) and a HIMU-type components (up to 20% in the mixing). The results of the mixing calculations are shown in Figs. 3, 4 and 6. Note that the mass balance models were performed in a binary way in these figures. Firstly, a mixing process between the DMM and EMI components was modeled, and then the result of the calculated composition was modeled with the third component (HIMU). The contributions of each component for this two-step binary mixture in the peridotitic source of the Davis Bank are calculated at DMM: 56%, EMI: 24%, and HIMU: 20%. For the other VTR occurrences, a less important EMI contribution is envisaged (Fig. 6).

5.4. *A genetic model for the Davis Bank source components*

In the preceding section, we concluded that the isotope

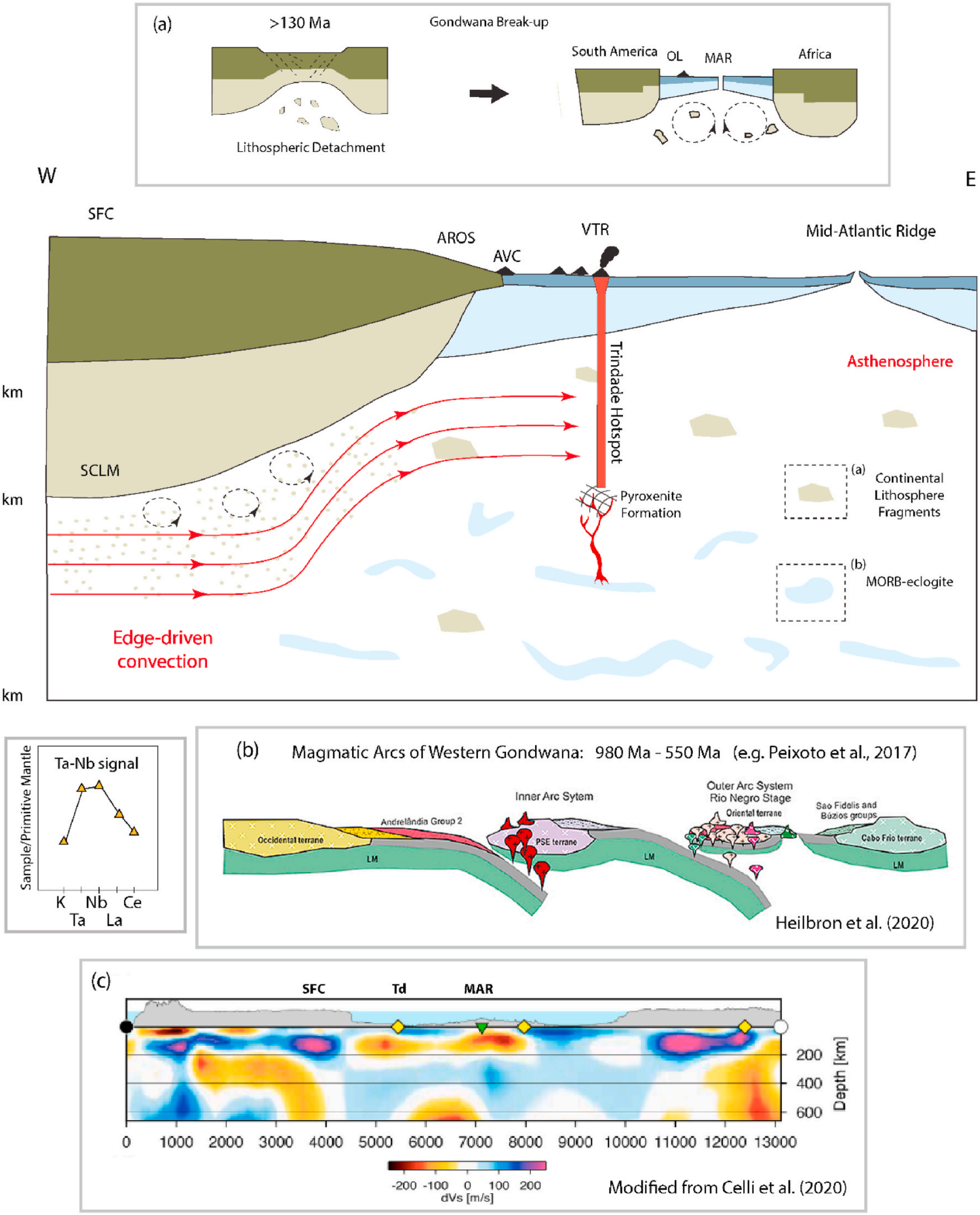

Fig. 7. Schematic sketch depicting the envisioned model for the three-component mantle source of the VTR magmatism, and the tectonic setting associated. The figure depicts edge-driven convection in the asthenosphere (King and Anderson, 1998) contributing to mantle heterogeneity and a hybridized (marble-cake) mantle (Allègre and Turcotte, 1986) with subcontinental lithosphere fragments (EMI) detached during the Gondwana breakup (Hawkesworth et al., 1986; Bizzi et al., 1995; Maia et al., 2021) and recycled slabs of oceanic lithosphere subducted during the Brasiliano Event and converted into MORB-eclogite, which reacts with the sub solidus peridotite forming pyroxenite (HIMU) (*e.g.,* Sobolev et al., 2005; Mallik and Dasgupta, 2012), embedded in the peridotitic mantle (DMM). The Ta–Nb signal of Davis Bank lava (sample V2410/5; Peyve and Skolotnev, 2014) showing a positive anomaly is depicted as evidence of recycled dehydrated subducted oceanic crust signature in the mantle source. (a) Tectonic model of continental lithosphere detachment during the Gondwana breakup sometime prior to 130 Ma and the South Atlantic Ocean opening during the Mesozoic; (b) Tectonic model from Heilbron et al. (2020) of subduction processes during the Brasiliano Event which resulted in the amalgamation of West Gondwana and involved multiple orogenic systems, such as the Araçuaí-Ribeira Orogenic System (AROS), which ages of magmatic arcs range from ca. 980 to 550 Ma (compilation from Peixoto et al., 2017); (c) W-E cross-sections tomographic image across the study area modified from Celli et al. (2020).

characteristics of the magmas that erupted along the VTR could be explained considering the mantle sources incorporating, in variable proportions, three end-members with features similar to those of the DMM, HIMU, and EMI mantle components. We envisage the mantle sources dominated by an asthenospheric component chemically similar to the DMM but hybridized by fluids and/or magmas related to recycling MORB-eclogite (HIMU) and originated from detached continental lithosphere (EMI).

The EMI component is ascribed to processes by which the Brazilian Neoproterozoic continental lithosphere was detached during the Mesozoic breakup of Africa and South America and remained in the asthenosphere (Hawkesworth et al., 1986; Bizzi et al., 1995; Maia et al., 2021). Indeed, the EMI component is commonly interpreted to have a shallow origin from the metasomatized delaminated subcontinental lithospheric mantle. The role of ancient subducted slabs during the Brasiliano Orogeny in the origin VTR isotopic enrichment has been recognized by several authors (Marques et al., 1999; Siebel et al., 2000; Bongiolo et al., 2015; Santos et al., 2018a; Maia et al., 2021) based on T_{DM} Nd model ages ranging from 420 to 640 Ma, which coincides with the Brasiliano Event. On the other hand, recent papers considers an alternative of deep origin for the EMI component (*e.g.*, Class and Le Roex, 2011).

Subducted slabs of Neoproterozoic oceanic lithosphere detached during the evolution of the Neoproterozoic-Cambrian Brasiliano/Pan-African Orogenic System have been incorporated into the upper mantle and contaminated the local mantle underneath the South Atlantic Ocean. The Brasiliano Event resulted in the amalgamation of West Gondwana and involved multiple orogenic systems (Fig. 7b) with partially coeval stages of subduction and collision (*e.g.*, Heilbron et al., 2020), including the Araçuaí-Ribeira Orogenic System (AROS, *e.g.,* Heilbron et al., 2017). Neoproterozoic Magmatic Arcs of Western Gondwana date from ca. 980 to 550 Ma (Peixoto et al., 2017; Heilbron et al., 2020), which means subduction may have started some time before that, and we speculate oceanic slabs may have up to 1.3 Ga. It is noteworthy that the sources of the northern Paraná basalts (Marques et al., 2018; Rocha-Júnior et al., 2020), several occurrences of small-volume ultramafic alkaline magmatism that surround the Paraná Basin, and some oceanic basalts in the South Atlantic, all appear to be related to the EMI component (Bizzi et al., 1995; Hawkesworth et al., 1986). As discussed by these authors, the oceanic basalts with EMI flavor in the South Atlantic are ascribed to processes by which the Brazilian Neoproterozoic continental lithosphere was delaminated and contaminated a zone of the South Atlantic asthenosphere. In addition to the Paraná basalts and alkaline rocks that border the Paraná Basin having EMI affinity, they also have similar Nd model ages, ranging from 0.8 to 1.3 Ga, indicating that the mantle source that gave rise to these rocks was metasomatized by slab-derived fluids of a mid-to late-Proterozoic event such as the Brasiliano. The isotopic and temporal overlapping of different magmatic events cannot be accidental and lead us to believe that these events were, directly or indirectly, affected by Neoproterozoic subduction processes (events of the Brasiliano/Pan-African orogenic cycle). Robust elemental and isotopic geochemistry data on Neoproterozoic plutonic and volcanic rocks of the Mantiqueira Province, including the Ribeira and Araçuaí belts, testifies to the consumption of an oceanic lithosphere to generate the orogeny (Caxito et al., 2021).

The HIMU signatures would be related to Neoproterozoic subduction processes in Western Gondwana, leading to the formation of several orogenic belts from the Brasiliano Event (*e.g.,* Heilbron et al., 2020). The origin of the HIMU signature in OIB magmas is commonly associated with mantle plumes carrying to the surface ancient recycled (>1Ga) oceanic crust (*e.g.*, White, 2015) that resided at deep levels of the mantle (*e.g.*, D″ layer; White, 2015). Based on geochemical and isotope data from VTR rocks, including Davis Bank, it seems likely that these rocks have been generated from a source consisting of different proportions of peridotite and olivine-poor components (*e.g.*, pyroxenite, garnet pyroxenite, or eclogite), which occur by partial melting of the MORB-eclogite and injection of its silicic melts into the surrounding mantle peridotite, yielding a 'hybrid pyroxenite'. Note that the high-TiO_2 contents of the Davis Bank rocks, along with the depletions in Rb, K, U, and Sr, plus positive anomalies of fluid-immobile incompatible elements like Nb and Ta (Fig. 7; Peyve and Skolotnev, 2014; Jesus et al., 2019) are robust evidence for signatures inherited from recycled oceanic crust in the mantle source, as well as a consequence of dehydration of oceanic crust during subduction (*e.g.*, Day et al., 2010; Hofman, 2014). The recycling of ocean crust inevitably leads to the transformation of basalt in eclogite through the typical low T/high P metamorphism at subduction zones. Gurenko et al. (2009) and Day et al. (2010), in explaining the petrogenesis of the HIMU-type Canary Islands lavas, demonstrated the role of MORB-eclogite, which when melted produced 'reaction pyroxenite'. It should be noted that an alternative model for the origin of HIMU signatures was proposed by Halliday et al. (1995) which suggested that HIMU-type signatures could also have a recent and shallow origin derived through the metasomatism of the oceanic lithospheric mantle. It is noteworthy that Halliday et al. (1992, 1995), based on Pb isotopes, attributed the HIMU component of the Trindade mantle source to young strong enrichments in U and Th relative to Pb.

Evidence for alkaline basaltic melts derived from pyroxenite fraction in the peridotite mantle (reaction between MORB-eclogite and *subsolidus* peridotite) can be statistically distinguished from peridotite-derived melts through a polynomial relationship of major element log-ratios called FCKANTMS marker, which is used to identify the source lithology for natural basalts (Yang et al., 2019). For instance, crustal material recycling and mantle metasomatism can result in mineralogical and compositional heterogeneities, producing a variety of mafic and ultramafic rocks, *e.g.*, metasomatized peridotite, pyroxenite, hornblendite. If we consider only Davis Bank rocks with MgO >10 wt% (sample V2410/10 from Peyve and Skolotnev, 2014), the FCKANTMS value is 0.27, which is higher than those melts derived from common peridotite. Hence, based on this statistical model in the log-ratio space, the source lithology of the Davis Bank should have been influenced by olivine-free pyroxenite.

5.5. On the origin of the Vitória-Trindade Ridge and the relation to South Atlantic tectonics

For the majority of researchers, the origin of the VTR is attributed to the effect of the South American Plate passing above the Trindade hotspot (*e.g.*, Gibson et al., 1995; VanDecar et al., 1995). However, even with our new age, it is clear that only sparse geochronological data have been published so far for the Vitória- Trindade Ridge, especially concerning seamounts and banks. Some authors use the supposed progressivity of the dated volcanic episodes to support the Trindade Plume hypothesis (*e.g.*, Skolotnev et al., 2011; Santos et al., 2021). However, besides the Trindade-Martin Vaz archipelago (ranging from 3.9 Ma to 0.17 Ma; Cordani, 1970; Pires et al., 2016; Santos et al., 2021) and Davis Bank, the only dated volcanic edifice by radioisotopic geochronology is the Jaseur Seamount (29.8 ± 6.6 Ma by U–Pb zircon method; Skolotnev et al., 2011), but the age obtained has a large uncertainty that can even overlap with the Davis Bank age and therefore make this result barely useable.

The lack of robust geochronological data on the seamounts and banks prevents thoroughly testing the idea of the VTR formation due to the passage of the lithosphere over a fixed plume in the mantle. Furthermore, the role of the Vitória-Trindade Fracture Zone in the ascent of the magma and evolution of the VTR cannot be overlooked (Barão et al., 2020; Alves et al., 2006), and its influence should be considered when discussing the genesis of the magmatic episodes. Only a larger precise and accurate geochronological data will be able to address if the age progression is entirely related to the movement of the plate, or if channeling of the magma through easy crustal pathways induces some level of randomness in the age progression.

The importance of structural control in the formation and evolution of this unique sub-latitudinal linear geological structure is clear (Ferrari and Riccomini, 1999; Barão et al., 2020). Indeed, for some authors, its development is related to the tectonic framework of the South Atlantic Ocean (Heine et al., 2013; Colli et al., 2014). During the Gondwana breakup and the opening of the South Atlantic Ocean, a system of fractures representing weakened zones of the lithosphere formed as, for instance, the Vitória-Trindade Fracture Zone (VTFZ), along which lies the Vitória-Trindade volcanic ridge (*e.g.,* Ferrari and Riccomini, 1999; Alves et al., 2006). Hence, one hypothesis about the formation of this volcanic ridge considers the role of the fracture zone as a conduit for the ascent of magmas generated in a sub-lithospheric thermal anomaly (*e.g.*, Alves et al., 2006). In this perspective, the existence of the Trindade Plume and the magnitude of this anomaly are controversial.

Although the origin of such alkaline magmatic episodes is still argued, the Vitória-Trindade Ridge reflects important Cenozoic oceanic tectonic-magmatic activity in this planet region. Several authors highlight the contemporaneity of alkaline intrusion and episodes of tectonic reactivation on the onshore Brazilian territory (*e.g.*, Cogné et al., 2012). The onshore emplacement of alkaline bodies during the Late Cretaceous and the Paleocene (Cogné et al., 2012), with emphasis on the Poços de Caldas – Cabo Frio Lineament has been linked to coeval tectonic uplift events in the Brazilian coast due to reactivation of the main intraplate structures (Fig. 4) such as the shear zones parallel to the coast and to transfer zones (*e.g.,* Souza et al., 2021).

The voluminous volcanic activity at the Davis Bank build-up may have started in the Oligocene (*ca.* 31 Ma), as suggested by Skolotnev et al. (2011), lasting for 10 Ma until Early Miocene. A tectonic reactivation on the Brazilian territory at this time is proposed. Japsen et al. (2012), Cogné et al. (2012) and Souza et al. (2021) interpreted a reactivation of transfer zones in the Neogene, marking an uplift phase starting approximately at the Oligo-Miocene boundary on NE and SE Brazil. Similarly, Cogné et al. (2012) highlight the increase in sediment supply during the Miocene in Campos and Santos basins as support for the Neogene fast cooling event recorded in samples from SE and NE Brazil (Cogné et al., 2012; Japsen et al., 2012).

Both tectonic events are synchronous to important tectonic episodes on a broader scale, leading some authors (*e.g.,* Meisling et al., 2001) to propose a correlation between them. For instance, the supposed Neogene uplift event in the Brazilian passive margin has also been linked to the Andes Orogeny as it coincides with the peak of the Andean uplift during the Quechuan Phase (25–0 Ma) (Cogné et al. 2012; Japsen et al., 2012). Japsen et al. (2012) suggest that the uplift experienced throughout Brazil during the Oligo-Miocene has a common cause with the Andean uplift and the increase in spreading velocity of the South Atlantic. Similarly, Colli et al. (2014) linked the two main phases of the Andes uplift, including the uplift peak during the Oligo-Miocene, to phases of fast-spreading rates of the South Atlantic, owing to an active role of the asthenospheric mantle causing dynamic topography and rapid plate motion velocity changes.

Indeed, this region corresponds to an anomalous positive dynamic topography (Cowie and Kusznir, 2018), indicating a hot mantle thermal structure or upwelling convection, as suggested by Stanton et al. (2021) for the Abrolhos Volcanic Complex (AVC). Moreover, Celli et al. (2020) observed through their tomographic model, strong low-velocity seismic wave anomaly under a large portion of the Vitoria-Trindade Ridge at depths of 100–250 km, which may indicate either anomalous hot asthenosphere or anomalous compositional contrasts. This seismic evidence shows little correlation to the concept of a classic narrow, deep-seated plume, yet a recent seismic tomographic study (Civiero et al., 2021) has shown, for the Canary/Morocco region a significant heterogeneity in the shape and lateral extension of mantle upwellings rooted in the Central-East Atlantic Anomaly stacked beneath the 660 km seismic discontinuity.

Nevertheless, tomographic images by Celli et al. (2020) depict a very complex and interconnected pattern of low-velocity anomalies in the mantle beneath the South Atlantic Ocean, apparently not existent beneath the 260 km depth. Also, the origin of the AVC is commonly linked to the VTR, due to its proximity, and attributed to the Trindade Plume (Thompson et al., 1998; Gibson et al., 1995; Siebel et al., 2000). Nevertheless, Stanton et al. (2021), based on extensive geophysical mapping using seismic reflection data, suggested magmatic activity affecting sediments as recent as the Middle Miocene and, thus, contemporary to the Davis Bank magmatic episode thus, also invalidating a link between the VTR and the AVC to a fixed Trindade Plume.

We further suggest that an analog for the VTR could be the Fernando de Noronha Island, where Knesel et al. (2011) and Perlingeiro et al. (2013) proposed such alkaline magmatism to be a manifestation of the upwelling flow from an edge-driven convection model (EDC, King and Anderson, 1998), rather than tracking passage over a deep-seated mantle plume. The EDC is an alternative model to the formation of some intraplate volcanism assumed to be formed above regions where differences in lithospheric thickness cause thermal contrasts driving small-scale convective flows (King and Anderson, 1998). According to Knesel et al. (2011), the Vitória-Trindade Ridge (VTR) is also geometrically favorable for the EDC mechanism.

To illustrate the envisioned origin of the enriched components of the VTR mantle source, Fig. 7 shows a hypothetical model with a hybridized mantle beneath the VTR and the tectonic events that may have led to the incorporation of fragments of recycled oceanic crust and subcontinental lithosphere into the local mantle, integrating models from different authors (King and Anderson, 1998; Allègre and Turcotte, 1986; Hawkesworth et al., 1986; Bizzi et al., 1995; Maia et al., 2021; Sobolev et al., 2005; Mallik and Dasgupta, 2012; Heilbron et al., 2020). The presence of such recycled materials at the convective mantle may account for the large, shallow, and interconnected pattern of seismic anomalies that have been observed underneath many intraplate volcanism regions across the South Atlantic (O'Connor et al., 2018; Celli et al., 2020). Although we acknowledge the occurrence of the EDC mechanism in the envisioned model for the genesis of the VTR due to the favorable geometry of the region, as pointed out by Knesel et al. (2011), we argue that such a mechanism cannot explain the formation of volcanic ridge aligned perpendicular to the coastline, since EDC is expected to sustain volcanism in an elongated zone that is parallel to the lithospheric boundary (Manjón-Cabeza Córdoba and Ballmer, 2021). The EDC in this scenario may only regionally contribute to the heterogeneity of the mantle through the process of lithospheric erosion. The presence of anomalous fertile sources (*e.g.*, pyroxenite) within an asthenosphere close to the melting point can account for the generation of a melting anomaly, rather than the need to invoke anomalously high temperatures (Lustrino, 2005). Such melting anomaly patches confined to the asthenospheric mantle would move slower than the overlying lithospheric plate, giving an illusion of a fixed hotspot (Anderson, 2005). The term hotspot here is used as the definition by Courtillot et al. (2003) of a Tertiary hotspot of shallow origin not related to deep mantle plumes.

6. Concluding remarks

(1) The combined Sr-Nd-Pb isotope data presented here suggest an isotopic variability for the VTR, mainly because of the more unradiogenic Nd isotopic ratios in Davis Bank samples, as also reported for Vitória Seamount samples, which challenges some interpretations about the homogeneity of the mantle source of the VTR. The enriched Sr-Nd-Pb signatures of both volcanic edifices preclude the generation of Davis Bank magma via exclusive melting of depleted mantle source and confirm the previous conjecture of several authors about the significant contribution of the EMI and HIMU mantle components in the source of the Vitória-Trindade Ridge magmatism. Data also suggest that those components evolved in an environment with low Sm/Nd and slightly high Rb/Sr, U/Pb, and Th/Pb ratios. Thus, the isotopic variations along the ridge could be explained by a heterogeneous

three-component mantle source (DMM, EMI, HIMU) with variable mixing proportions.

(2) Modeling of the isotopic data suggests that the best fit in terms of Nd, Pb, and Sr isotopic composition is achieved by partial melting of a depleted mantle represented by a dominant asthenospheric component (DMM) hybridized by the addition of EMI ($<$24% in the mixing) and HIMU (up to 20% in the mixture) melts.

(3) The three isotopically different mantle components identified here may be explained by a lithologically heterogeneous mantle. The origin of the EMI component in the source of the magmatism studied can be attributed to detached metasomatized fragments of subcontinental lithospheric mantle slabs left at shallow levels, as previously suggested by Marques et al. (1999). As an alternative to the hypothesis of the HIMU mantle component in the VTR source characterized as a deep mantle material ascending from a plume, we believe in a model with ubiquitous heterogeneities in a depleted mantle matrix, in which the Brasiliano Orogeny played a significant role regarding the incorporation of enriched materials into the mantle. Recycled slabs of Neoproterozoic oceanic lithosphere subducted during the Brasiliano Event, converted into MORB-eclogite, may have contaminated the local mantle underneath the Vitória-Trindade Ridge. We invoke a HIMU-type pyroxenite formed by partial melting of the MORB-eclogite and injection of its silicic melts into the surrounding mantle peridotite.

(4) The $^{40}Ar/^{39}Ar$ dating of one tephrite sample from Davis Bank yielded a mini *plateau* age of 21.42 ± 0.13 Ma, corroborating the previously published ages, altogether suggesting a dominant edifice-building episode at *ca.* 21 Ma. Such an age points toward a volcanic age progression along the VTR, which is one of the pieces of evidence that support the Trindade Hotspot hypothesis. However, this hypothesis should be properly tested as very few robust geochronological data have been published so far. In addition, the role of the structural control in the evolution of this linear ridge should not be overlooked, and additional geochronological data are necessary to properly test the role of such structural control in channeling magma to the surface.

Funding

This work was supported by the CNPq (Pro Trindade Program) [Process N∘. 557,146/2009–7]; the MCT/CNPq project [n∘ 26/2009]; the Universidade do Estado do Rio de Janeiro for PROCAD Program (Capacitation Program) leave and CAPES [Process 88,881.177228/2018–01]; and FAPERJ [APQ1 2019 n 210.179/2019]. Also support from the scientific scholarships PROCIENCIA UERJ 2020, PQ CNPq 2022 and JCNE FAPERJ 2022.

CRediT authorship contribution statement

Gabriella de Oliveira Amaral Quaresma: Writing – review & editing, Writing – original draft, Methodology, Conceptualization. **Anderson Costa dos Santos:** Writing – review & editing, Validation, Resources, Project administration, Methodology, Funding acquisition, Formal analysis, Conceptualization. **Eduardo Reis Viana Rocha-Júnior:** Writing – review & editing, Validation, Software, Conceptualization. **Juliana Bonifácio:** Software. **Caio Assumpção Queiroz Rego:** Writing – review & editing. **João Mata:** Writing – review & editing, Methodology, Formal analysis. **Claudio de Morisson Valeriano:** Writing – review & editing, Methodology. **Fred Jourdan:** Writing – review & editing, Methodology, Formal analysis. **Nadine Mattielli:** Methodology, Formal analysis. **Mauro César Geraldes:** Project administration, Funding acquisition.

Declaration of competing interest

The authors declare that they have no known competing financial interests or personal relationships that could have appeared to influence the work reported in this paper.

Data availability

Data will be made available on request.

Acknowledgments

The authors thank the CNPq (Pro Trindade Program) for the support to this research (Process Nº. 557146/2009–7), the logistic support of the Brazilian Navy. We thank LAGIR staff for support and isotope analyzes. The present work is linked to the MCT/CNPq project n° 26/2009, under the coordination of researchers from Rio de Janeiro State University (UERJ) and cooperation from Federal University of Rio de Janeiro (UFRJ). We thank Universidade do Estado do Rio de Janeiro for supporting the second author Dr. Anderson Costa dos Santos, through its PROCAD Program (Capacitation Program) and CAPES Process 88881.177228/2018–01 for the postdoctoral fellowship, to execute part of this research at Aveiro University, Portugal. We are very grateful to the Brazilian Navy LEPLAC Program staff, especially Captain Izabel King Jack and Captain Ana Angélica Ligiero Alberoni for the support and for sharing the dredged rocks from LEPLAC Program with our Geology Faculty team and for allowing the use of the bathymetric data set, as well as to the technical group that has been studying the Brazilian Continental Margin since 1987 in order to produce the Brazilian Submission for the extension of the Continental Shelf according to Article 76 of UNCLOS. Our many thanks to Dr. Fred Jourdan (Curtin University) for the $^{40}Ar/^{39}Ar$ analysis and for enlightening our discussions and to Prof. Dr. João Mata (Dom Luiz Research Group) for supporting the Pb–Hf analysis in partnership with Dr[a]. Nadine Mattielli (Université Libre de Bruxelles). Dr. Anderson Costa dos Santos would like to dedicate this manuscript to Prof. Ronald Viktor Fodor from NCSU for encouraging him in the Alkaline offshore volcanism and supporting his research and career. Dr. Fodor passed away in October 22nd, 2021 and he will be always remembered throughout Dr. Santos professional life. In name of our research group, we pay this tribute to one of the greatest known petrologist.

Appendix A. Supplementary data

Supplementary data to this article can be found online at https://doi.org/10.1016/j.jsames.2022.104099.

References

Alberoni, A.A.L., Jeck, I.K., Silva, C.G., et al., 2020. The new Digital Terrain Model (DTM) of the Brazilian Continental Margin: detailed morphology and revised undersea feature names. Geo-Mar Lett 40, 949–964. https://doi.org/10.1007/s00367-019-00606-x.

Allègre, C.J., Turcotte, D.L., 1986. Implications of a two-component marble-cake mantle. Nature 323, 123–127.

Alves, E.C., Araujo, R.S., Ramos, E.C., Maia, M., Santos, A.C, Hackspacher, P.C., 2022. Ocean fracture zones: their evolution and impact on tectonic and magmatism of the South and Southeast Brazilian continental margin. Meso-Cenozoic Brazilian Offshore Magmatism. Academic Press, pp. 47–94. ISBN 9780128239889.

Alves, E.C., Maia, M., Sichel, S.E., Campos, C.M.P., 2006. Zona de Fratura de Vitória-Trindade no Atlântico Sudeste e suas implicações tectônicas. Rev. Bras. Geofís. 24, 117–127.

Anderson, D.L., 2005. Large igneous provinces, delamination, and fertile mantle. Elements 1 (5), 271–275. https://doi.org/10.2113/gselements.1.5.271.

Barão, L.M., Trzaskos, B., Angulo, R.J., De Souza, M.C., Daufenbach, H.F., Santos, F.A., Vasconcellos, E.M.G., 2020. Deformational structures developed in volcanic sequences as a product of tectonic adjustments in the South Atlantic Ocean. J. S. Am. Earth Sci. 104, 102812 https://doi.org/10.1016/j.jsames.2020.102812.

Bizzi, L.A., De Wit, M.J., Smith, C.B., McDonald, I., Armstrong, R.A., 1995. Heterogeneous enriched mantle materials and Dupal-type magmatism along the SW

margin of the São Francisco craton, Brazil. J. Geodyn. 20 (4), 469–491. https://doi.org/10.1016/0264-3707(95)00028-8.
Bongiolo, E.M., Pires, G.L.C., Geraldes, M.C., Santos, A.C., Neumann, R., 2015. Geochemical modeling and Nd-Sr data links nephelinite-phonolite successions and xenoliths of Trindade Island (South Atlantic Ocean, Brazil). J. Volcanol. Geoth. Res. 306, 58–73. https://doi.org/10.1016/j.jvolgeores.2015.10.002.
Caxito, F.A., Heilbron, M., Valeriano, C.M., Bruno, H., Pedrosa-Soares, A., Alkmim, F.F., et al., 2021. Integration of elemental and isotope data supports a neoproterozoic adamastor ocean realm. Geochemical Perspective Letters 17, 6–10.
Celli, N.L., Lebedev, S., Schaeffer, A.J., Ravenna, N., Gaina, C., 2020. The upper mantle beneath the South Atlantic Ocean. South America and Africa from waveform tomography with massive data sets. Geophys. J. Int. 221, 178–204. https://doi.org/10.1093/gji/ggz574.
Chaffey, D.J., Cliff, R.A., Wilson, B.M., 1989. Characterization of the St. Helena source. In: Saunders, A.D., Norry, M.J. (Eds.), Magmatism in the Ocean Basins. Geological Society, London, Special Publications, pp. 257–276. https://doi.org/10.1144/GSL.SP.1989.042.01.16.
Civiero, C., Custódio, S., Neres, M., Schlaphorst, D., Mata, J., Silveira, G., 2021. The role of the seismically slow Central-East Atlantic Anomaly in the genesis of the Canary and Madeira volcanic provinces. Geophys. Res. Lett. 48, e2021GL092874 https://doi.org/10.1029/2021GL092874.
Class, C., le Roex, A., 2011. South Atlantic DUPAL anomaly — dynamic and compositional evidence against a recent shallow origin. Earth Planet Sci. Lett. 305, 92–102. https://doi.org/10.1016/j.epsl.2011.02.036. Issues 1–2.
Cogné, N., Gallagher, K., Cobbold, P.R., Riccomini, C., Gautheron, C., 2012. Post-breakup tectonics in southeast Brazil from thermochronological data and combined inverseforward thermal history modeling. J. Geophys. Res. 117, B11413 https://doi.org/10.1029/2012JB009340.
Colli, L., Stotz, I., Bunge, H.P., Smethurst, M., Clark, S., Iaffaldano, G., Tassara, A., Guillocheau, F., Bianchi, M.C., 2014. Rapid South Atlantic spreading changes and coeval vertical motion in surrounding continents: evidence for temporal changes of pressure-driven upper mantle flow. Tectonics 33, 1304–1321. https://doi.org/10.1002/2014TC003612.
Conrad, C.P., Lithgow-Bertelloni, C., 2006. Influence of continental roots and asthenosphere on plate-mantle coupling. Geophys. Res. Lett. 33, L05312 https://doi.org/10.1029/2005GL025621.
Cordani, U.G., 1970. Idade Do Vulcanismo Do Oceano Atlântico Sul, vol. 1. Boletim do Instituto de Geociências e Astronomia (IGA-USP), pp. 9–75.
Cordani, U.G., Ramos, V.A., Fraga, L.M., Cegarra, M., Delgado, I., Souza, K.G.D., Schobbenhaus, C., 2016. Tectonic Map of South America. CGMW-CPRM-SEGEMAR. http://rigeo.cprm.gov.br/jspui/handle/doc/16750.
Courtillot, V., Davaille, A., Besse, J., Stock, J., 2003. Three distinct types of hotspots in the Earth's mantle. Earth and Planetary Science Letters 205 (3–4), 295–308. https://doi.org/10.1016/S0012-821X(02)01048-8. ISSN 0012-821X.
Cowie, L., Kusznir, N., 2018. Renormalisation of global mantle dynamic topography predictions using residual topography measurements for "normal" oceanic crust. Earth Planet Sci. Lett. 499 (3), 145–156. https://doi.org/10.1016/j.epsl.2018.07.018.
Day, J.M.D., Pearson, D.G., Macpherson, C.G., Lowry, D., Carracedo, J.C., 2010. Evidence for distinct proportions of subducted oceanic crust and lithosphere in HIMU-type mantle beneath El Hierro and La Palma, Canary Islands. Geochem. Cosmochim. Acta 74, 6565–6589. https://doi.org/10.1016/j.gca.2010.08.021.
DePaolo, D.J., Wasserburg, G.J., 1979. Neodymium isotopes in flood basalts from the Siberian Platform and inferences about their mantle sources. Proceed Nat Acad Sci 76 (6), 3056–3060.
Ferrari, A., Riccomini, C., 1999. Campo de esforços Plio Pleistocênico na Ilha de Trindade (Oceano Atlântico Sul, Brasil) e sua relação com a tectônica regional. Rev. Bras. Geociencias 29, 195–202.
Fodor, R.V., Hanan, B.B., 2000. Geochemical evidence for the Trindade Hotspot trace: columbia seamount ankaramite. Lithos 51, 293–304. https://doi.org/10.1016/S0024-4937(00)00002-5.
Fodor, R.V., McKee, E.H., Asmus, H.E., 1983. K-Ar ages and the opening of the South Atlantic Ocean: basaltic rock from the Brazilian margin. Mar. Geol. 54 https://doi.org/10.1016/0025-3227(83)90002-6. M1–M8.
Fodor, R.V., Mukasa, S.B., Gomes, C.B., Cordani, U.G., 1989. Ti-rich eocene basaltic rocks, abrolhos platform, Offshore Brazil, 18∘S: petrology with respect to South Atlantic magmatism. J. Petrol. 30, 763–786. https://doi.org/10.1093/petrology/30.3.763.
Galer, S.J.G., Abouchami, W., 1998. Pratical application of lead triple spiking for correction of instrumental mass discrimination. Mineral. Mag. 62 (A), 491–492.
Gibson, S.A., Thompson, R.N., Leonardos, O.H., Dickin, A.P., Mitchell, J.G., 1995. The Late Cretaceous impact of the Trindade mantle plume: evidence from large-volume, mafic, potassic magmatism in SE Brazil. J. Petrol. 36, 189–229. https://doi.org/10.1093/petrology/36.1.189.
Gurenko, A.A., Sobolev, A.V., Hoernle, K.A., Hauff, F., Schmincke, H.U., 2009. Enriched, HIMU-type peridotite and depleted recycled pyroxenite in the Canary plume: a mixed-up mantle. Earth Planet Sci. Lett. 277, 514–524.
Halliday, A.N., Davies, G.R., Lee, D.C., Tommasini, S., Oaslick, C.R., Fitton, J.G., James, D.E., 1992. Lead isotope evidence for young trace element enrichment in the oceanic upper mantle. Nature 359, 623–627. https://doi.org/10.1038/359623a0.
Halliday, A.N., Lee, D.C., Tommasini, S., Davies, G.R., Paslick, C.R., Fitton, G.J., James, D.E., 1995. Incompatible trace elements in OIB and MORB and source enrichment in the sub-oceanic mantle. Earth Planet Sci. Lett. 133, 379–395.
Hart, S.R., 1988. Heterogeneous mantle domains: signatures, genesis and mixing chronologies. Earth Planet Sci. Lett. 90, 272–296. https://doi.org/10.1016/0012-821X(88)90131-8.
Hawkesworth, C.J., Mantovani, M.S.M., Taylor, P.N., Palacz, Z., 1986. Evidence from the Paraná of south Brazil for a continental contribution to Dupal basalts. Nature 322, 356–359. https://doi.org/10.1038/322356a0.
Heilbron, M., Tupinambá, M., Valeriano, C.M., Armstrong, R., Eirado, L.G.S., Melo, R.S., Simonetti, A., Soares, A.C.P., Machado, N., 2013. The Serra da Bolívia Complex: the record of a new Neoproterozoic arc-related unit at Ribeira belt. Precambrian Res. 238, 158–175. https://doi.org/10.1016/j.precamres.2013.09.014.
Heilbron, M., Cordani, U.G., Alkmim, F.F., Reis, H.L.S., 2017. Tectonic genealogy of a miniature continent. Springer, Regional Geological Reviews. In: Heilbron, M., Cordani, U., Alkmim, F. (Eds.), The São Francisco Craton and its Margins: Tectonic Genealogy of a Miniature Continent 17, 321–331. https://doi.org/10.1007/978-3-319-01715-0_17.
Heilbron, M., Valeriano, C.M., Peixoto, C., Tupinambá, M., Neubauer, F., Dussin, I., Corrales, F., Bruno, H., Lobato, M., Almeida, J.C.H., Silva, L.G.E., 2020. Neoproterozoic magmatic arc systems of the central Ribeira belt, SE-Brazil, in the context of the West-Gondwana pre-collisional history: a review. J. S. Am. Earth Sci. 102710. https://doi.org/10.1016/j.jsames.2020.102710.
Heine, C., Zoethourt, J., Muller, R.D., 2013. Kinematics of the South atlantic rift. Solid Earth 4, 215–253. https://doi.org/10.5194/se-4-215-2013.
Hofman, A.W., 2014. 3.3 -. In: Holland, H.D., Turekian, K.K. (Eds.), Sampling Mantle Heterogeneity through Oceanic Basalts: Isotopes and Trace Elements, Treatise on Geochemistry, second ed., vol. 3, pp. 67–101. https://doi.org/10.1016/B978-0-08-0959757.00203-5.
Jackson, M.G., Dasgupta, R., 2008. Compositions of HIMU, EM1, and EM2 from global trends between radiogenic isotopes and major elements in ocean island basalts. Earth Planet Sci. Lett. 276, 175–186. https://doi.org/10.1016/j.epsl.2008.09.023.
Japsen, P., Bonow, J.M., Green, P.F., Cobbold, P.R., Chiossi, D., Lilletveit, R., Magnavita, L.P., Pedreira, A., 2012. Episodic burial and exhumation in NE Brazil after opening of the South Atlantic. Bull. Geol. Soc. Am. 124, 800–816. https://doi.org/10.1130/B30515.1.
Jesus, J.V.M., Santos, A.C., Mendes, J.C., Santos, W.H., Rego, C.A.Q., Geraldes, M.C., 2019. Petrogênese do Banco Davis, Cadeia Vitória-Trindade, Atlântico Sul: o Papel de Voláteis (H2O e CO2) na Evolução Magmática do Banco Davis. Anu. do Inst. Geociencias 42, 237–253. https://doi.org/10.11137/2019_3_237_253.
King, S.D., Anderson, D.L., 1998. Edge-driven convection. Earth Planet Sci. Lett. 160, 289–296. https://doi.org/10.1016/S0012-821X(98)00089-2.
Knesel, K.M., de Souza, Z.S., Vasconcelos, P.M., Cohen, B.E., Silveira, F.V., 2011. $^{40}Ar/^{39}Ar$ geochronology reveals the youngest volcanism in mainland Brazil and no evidence for a plume trace on the continent. Earth Planet Sci. Lett. 302, 38–50.
Koppers, A.A.P., 2002. ArArCALC-software for 40Ar/39Ar age calculations. Comput. Geosci. 28 (5), 605–619. https://doi.org/10.1016/S0098-3004(01)00095-4.
Lee, J.Y, Marti, K., Severinghaus, J.P., Kawamura, K., Yoo, H-S., Lee, J.B., Kim, J.S., 2006. A redetermination of the isotopic abundances of atmospheric Ar. Geochimica et Cosmochimica Acta 70 (17), 4507–4512. https://doi.org/10.1016/j.gca.2006.06.1563. ISSN 0016-7037.
Lustrino, M., 2005. How the delamination and detachment of lower crust can influence basaltic magmatism. Earth Sci. Rev. 72, 21–38. https://doi.org/10.1016/j.earscirev.2005.03.004.
Maia, T.M., Santos, A.C., Rocha-Júnior, E.R.V., Valeriano, C.M., Mendes, J.C., Jeck, I.K., Santos, W.H., Oliveira, A.L., Mohriak, W.U., 2021. First petrologic data for Vitória seamount, Vitória-Trindade Ridge, South Atlantic: a contribution to the trindade mantle plume evolution. Journal of S. Am. Earth Sci.,V. 109, 103304 https://doi.org/10.1016/j.jsames.2021.103304.
Maia, T.M., Santos, A.C., Valente, S.C., Rocha-Júnior, E.R.V., Barros, G.P.W., Heilbron, M., Valeriano, C.M., Arena, M., 2022. Abrolhos magmatic province petrogenesis and its link with the Vitória-Trindade Ridge, southeast Brazilian margin, South Atlantic ocean. J. S. Am. Earth Sci. 104075. https://doi.org/10.1016/j.jsames.2022.104075. ISSN 0895-9811.
Mallik, A., Dasgupta, R., 2012. Reaction between MORB-eclogite derived melts and fertile peridotite and generation of ocean island basalts. Earth Planet Sci. Lett. 329–330, 97–108.
Manjón-Cabeza Córdoba, A., Ballmer, M.D., 2021. The role of edge-driven convection in the generation of volcanism – Part 1: a 2D systematic study. Solid Earth 12, 613–632. https://doi.org/10.5194/se-12-613-2021.
Marques, L.S., Ulbrich, M.N.C., Ruberti, E., Tassinari, C.G., 1999. Petrology, geochemistry and Sr-Nd isotopes of the trindade and Martin Vaz volcanic rocks (southern Atlantic Ocean). J. Volcanol. Geoth. Res. 93, 191–216. https://doi.org/10.1016/S0377-0273(99)00111-0.
Marques, L.S., De Min, A., Rocha-Júnior, E.R.V., Babinski, M., Bellieni, G., Figueiredo, A.M.G., 2018. Elemental and Sr-Nd-Pb isotope geochemistry of the florianópolis dyke swarm (Paraná magmatic province): crustal contamination and mantle source constraints. J. Volcanol. Geoth. Res. 355, 149–164.
Meisling, K.E., Cobbold, P.R., Mount, V.S., 2001. Segmentation of an obliquely rifted margin, Campos and Santos basins, southeastern Brazil. AAPG (Am. Assoc. Pet. Geol.) Bull. 85, 1903–1924. https://doi.org/10.1306/8626D0A9-173B-11D7-8645000102C1865D.
Mohriak, W.U., 2005. Interpretação geológica e geofísica da Bacia do Espírito Santo e da região de Abrolhos: petrografia, datação radiométrica e visualização sísmica das rochas vulcânicas. Bol. Geociencias Petrobras 14, 133–142.
Monteiro, L.G.P., Santos, A.C., Pires, G.L.C., Barão, L.M., Rocha-Júnior, E.R.V., Biancini, J.R.C., Hackspacher, P.C., Júnior, H.I.A., Jeck, I.K., Santos, J.F., 2021. Chapter 10 - trindade Island: evolution of the geological knowledge. In: Hackspacher, P.C., Santos, A.C. (Eds.), Meso-Cenozoic Brazilian Offshore Magmatism: Geochemistry, Petrology and Tectonics. Elsevier Inc., pp. 337–390. https://doi.org/10.1016/B978-0-12-823988-9.00015-0

Motoki, A., Motoki, K.F., Melo, D.P., 2012. Submarine morphology characterization of the Vitória-Trindade Chain and the adjacent areas, state of Espírito Santo, Brazil, based on the predicted bathymetry of the TOPO version 14.1. Rev. Brasil. Geomorfol. 13, 151–170. https://doi.org/10.20502/rbg.v13i2.195.

Muller, R.D., Sdrolias, M., Gaina, C., Roest, W.R., 2008. Age, spreading rates, and spreading asymmetry of the world's ocean crust. G-cubed 9, Q04006. https://doi.org/10.1029/2007GC001743.

O'Connor, J.M., Jokat, W., Wijbrans, J.R., Colli, L., 2018. Hotspot tracks in the South Atlantic located above bands of fast flowing asthenosphere driven by waning pulsations from the African LLSVP. Gondwana Res. 53, 197–208.

Peixoto, C.A., Heilbron, M., Ragatky, D., Armstrong, R., Dantas, E., Valeriano, C.M., Simonetti, A., 2017. Tectonic evolution of the Juvenile Tonian Serra da Prata magmatic arc in the Ribeira belt, SE Brazil: implications for early west Gondwana amalgamation. Precambrian Res. 302, 221–254.

Perlingeiro, G., Vasconcelos, P.M., Knesel, K.M., Thiede, D.S., Cordani, U.G., 2013. $^{40}Ar/^{39}Ar$ geochronology of the Fernando de Noronha Archipelago and implications for the origin of alkaline volcanism in the NE Brazil. J. Volcanol. Geoth. Res. 249, 140–154. https://doi.org/10.1016/j.jvolgeores.2012.08.017.

Peyve, A.A., Skolotnev, S.G., 2014. Systematic variations in the composition of volcanic rocks in tectono-magmatic seamount chaines in the Brazil Basin. Geochem. Int. 52, 111–130. https://doi.org/10.1134/S0016702914020062.

Pilet, S., Baker, M.B., Muntener, O., Stolper, E.M., 2011. Monte Carlo simulations of metasomatic enrichment in the lithosphere and implications for the source of alkaline basalts. J. Petrol. 52, 1415–1442. https://doi.org/10.1093/petrology/egr007.

Pires, G.L.C., Bongiolo, E.M., 2016. The nephelinitic–phonolitic volcanism of the Trindade Island (South Atlantic Ocean): review of the stratigraphy, and inferences on the volcanic styles and sources of nephelinites. J. S. Am. Earth Sci. 72, 49–62. https://doi.org/10.1016/j.jsames.2016.07.008.

Pires, G.L.C., Bongiolo, E.M., Geraldes, M.C., Renac, C., Santos, A.C., Jourdan, F., Neumann, R., 2016. New $^{40}Ar/^{39}Ar$ ages and revised $^{40}K/^{40}Ar^*$ data from nephelinitic–phonolitic volcanic successions of the Trindade Island (South Atlantic Ocean). J. Volcanol. Geoth. Res. 327, 531–538. https://doi.org/10.1016/j.jvolgeores.2016.09.020.

Renne, P.R., Mundil, R., Balco, G., Min, K., Ludwig, K.R., 2010. Joint determination of ^{40}K decay constants and $^{40}Ar^*/^{40}K$ for the Fish Canyon sanidine standard, and improved accuracy for $^{40}Ar/^{39}Ar$ geochronology. Geochem. Cosmochim. Acta 74, 5349–5367. https://doi.org/10.1016/j.gca.2010.06.017.

Renne, P.R., Balco, G., Ludwig, K.R., Mundil, R., Min, K., 2011. Response to the comment by W.H. Schwarz et al. on "Joint determination of K-40 decay constants and Ar-40*/K-40 for the Fish Canyon sanidine standard, and improved accuracy for Ar- 40/Ar-39 geochronology" by Renne et al, 2010 Geochem. Cosmochim. Acta 75, 5097–5100. https://doi.org/10.1016/j.gca.2011.06.021.

Rocha-Júnior, E.R.V., Marques, L.S., Babinski, M., Machado, F.B., Petronilho, L.A., Nardy, A.J.R., 2020. A telltale signature of Archean lithospheric mantle in the Paraná continental flood basalts genesis. Lithos 364–365, 105519. https://doi.org/10.1016/j.lithos.2020.105519.

Rocha-Júnior, E.R.V., Marques, L.S., Babinski, M., Nardy, A.J.R., Figueiredo, A.M.G., Machado, F.B., 2013. Sr-Nd-Pb isotopic constraints on the nature of the mantle sources involved in the genesis of the high-Ti tholeiites from Northern Paraná Continental Flood Basalts (Brazil). J. S. Am. Earth Sci. 46, 9–25.

Salters, V.J.M., Stracke, A., 2004. Composition of the depleted mantle. G-cubed 5, Q05B07. https://doi.org/10.1029/2003GC000597.

Santos, A.C., 2016. Petrology of Martin Vaz Island and Vitoria-Trindade Ridge Seamounts: Montague, Jaseur, Davis, Dogaressa and Columbia. Trace Elements, $^{40}Ar/^{39}Ar$ Dating and Sr and Nd Isotope Analysis Related to the Trindade Plume Evidence. Ph. D. Thesis. Universidade do Estado do Rio de Janeiro, Brazil.

Santos, A.C., Hackspacher, P.C., 2021. Meso-Cenozoic Brazilian Offshore Magmatism: Geochemistry, Petrology and Tectonics. Elsevier Inc. Academic Press, p. 512. https://doi.org/10.1016/C2019-0-05400-3.

Santos, A.C., Geraldes, M.C., Siebel, W., Mendes, J., Bongiolo, E., Santos, W.H., Garrido, T.C.V., Rodrigues, S.W.O., 2018a. Pleistocene alkaline rocks of Martin Vaz volcano, South Atlantic: low-degree partial melts of a CO2-metasomatized mantle plume. Int. Geol. Rev. 61, 296–313. https://doi.org/10.1080/00206814.2018.1425921.

Santos, A.C., Mohriak, W.U., Geraldes, M.C., Santos, W.H., Ponte-Neto, C.F., Stanton, N., 2018b. Compiled potential field data and seismic surveys across the Eastern Brazilian continental margin integrated with new magnetometric profiles and stratigraphic configuration for Trindade Island, South Atlantic, Brazil. Int. Geol. Rev. 61, 1728–1744. https://doi.org/10.1080/00206814.2018.1542634.

Santos, A.C., Mata, J., Jourdan, F., Rodrigues, S.W. de O., Monteiro, L.G.P., Guedes, E., Benedini, L., Geraldes, M.C., 2021. Martin Vaz island geochronology: constraint on the Trindade Mantle Plume track from the youngest and easternmost volcanic episodes. J. S. Am. Earth Sci. 106, 103090 https://doi.org/10.1016/j.jsames.2020.103090.

Santos, A.C., Oliveira, O.L., Bevilaqua, L.A., Rocha-Júnior, E.R.V., Rodrigues, S.W.O., Mendes, J.C., Jeck, I.K., 2022a. Chapter 11 - Martin Vaz archipelago: the youngest magmatism in the Brazilian territory, 2021. In: Santos, A.C., Hackspacher, P.C. (Eds.), Meso-Cenozoic Brazilian Offshore Magmatism: Geochemistry, Petrology and Tectonics. Elsevier Inc., pp. 391–432. https://doi.org/10.1016/B978-0-12-823988-9.00013-7

Santos, A.C., Rocha-Júnior, E.R.V., Quaresma, G.O.A., Maia, T.M., Jesus, J.V.M., Rego, C.A.Q., Jeck, I.K., 2022b. Chapter 9 - vitória-Trindade seamounts: undersaturated alkaline series evolution from an enriched metasomatized source, 2021. In: Santos, A.C., Hackspacher, P.C. (Eds.), Meso-Cenozoic Brazilian Offshore Magmatism: Geochemistry, Petrology and Tectonics. Elsevier Inc., pp. 293–336. https://doi.org/10.1016/B978-0-12-823988-9.00004-6

Sharp, W.D., Renne, P.R., 2005. The 40Ar/39Ar dating of core recovered by the Hawaii Scientific Drilling Project (phase 2), Hilo, Hawaii. G-cubed 6 (4), Q04G17. https://doi.org/10.1029/2004GC000846.

Siebel, W., Becchio, R., Volker, F., Hansen, M.A.F., Viramonte, J., Trumbull, R.B., Haase, G., Zimmer, M., 2000. Trindade and Martin Vaz islands, South Atlantic: isotopic (Sr, Nd, Pb) and trace element constraints on plume related magmatism. J. S. Am. Earth Sci. 13, 79–103. https://doi.org/10.1016/S0895-9811(00)00015-8.

Skolotnev, S.G., Peive, A.A., 2017. Composition, structure, origin, and evolution of offaxis linear volcanic structures of the Brazil Basin, South Atlantic. Geotectonics 51, 53–73. https://doi.org/10.1134/S001685211701006X.

Skolotnev, S.G., Bylinskaya, M.E., Golovina, L.A., Ipateva, I.S., 2011. First data on the age of rocks from the central part of the Vit'oria–Trindade Ridge (Brazil basin, South Atlantic). Dokl. Earth Sci. 437, 316–322. https://doi.org/10.1134/S1028334X11030093.

Sobolev, A.V., Hofmann, A.W., Sobolev, S.V., Nikogosian, I.K., 2005. An olivine-free mantle source of Hawaiian shield basalts. Nature 434, 590–597. https://doi.org/10.1038/nature03411.

Souza, D.H., Hackspacher, P.C., Silva, B.V., Siqueira-Ribeiro, M.C., Hiruma, S.T., 2021. Temporal and spatial denudation trends in the continental margin of southeastern Brazil. J. S. Am. Earth Sci. 105, 102931 https://doi.org/10.1016/j.jsames.2020.102931, 9811.

Stanton, N., Gordon, A., Cardozo, C., Kusznir, N., 2021. Morphostructure, emplacement and duration of the Abrolhos Magmatic Province: a geophysical analysis of the largest post-breakup magmatism of the South-Eastern Brazilian margin. Mar. Petrol. Geol. 133, 105230 https://doi.org/10.1016/j.marpetgeo.2021.105230.

Stracke, A., Hofmann, A.W., Hart, S.R., 2005. FOZO, HIMU, and the rest of the mantle zoo. G-cubed 6, Q05007. https://doi.org/10.1029/2004GC000824.

Sun, S.-s., McDonough, W.F., 1989. Chemical and isotopic systematics of ocean basalts; implications for mantle composition and processes. Geol. Soc. Lond. Special Publ. 42, 313–345.

Tanaka, T., Togashi, S., Kamioca, H., 2000. JNd-1: a Neodymium isotopic reference in consistency with La Jolla Neodymium. Chem. Geol. 168, 279–281. https://doi.org/10.1016/S0009-2541(00)00198-4.

Thompson, R.N., Gibson, S.A., Mitchell, J.G., Dickin, A.P., Leonardos, O.H., Brod, J.A., Greenwood, J.C., 1998. Migrating cretaceous – eocene magmatism in the Serra do mar alkaline province, SE Brazil: melts from the deflected trindade mantle plume? J. Petrol. 39, 1493–1526. https://doi.org/10.1093/petroj/39.8.1493.

Valeriano, C.M., Ragatk, C.D., Geraldes, M.C., Heilbron, M., Valladares, C.S., Schmitt, R. S., Tupinambá, M., Palermo, N., Almeida, J.C.H., Duarte, B.P., Martins, J.R.E., Nogueira, J.R., 2003. A new TIMS laboratory under construction in Rio de Janeiro, Brazil. In IV south American symposium on isotope geology, salvador. Short Papers IV South Am. Symp. Isotope Geol. 1, 131–133.

Vandecar, J.C., James, D.E., Assumpcao, M., 1995. Seismic evidence for a fossil mantle plume beneath SouthAmerica and implications for plate driving forces. Nature 378, 25–31.

White, W.M., 2015. Isotopes, DUPAL, LLSVPs, and anekantavada. Chem. Geol. 419, 10–28.

Workman, R.K., Hart, S.R., 2005. Major and trace element composition of the depleted MORB mantle (DMM). Earth Planet Sci. Lett. 231, 53–72. https://doi.org/10.1016/j.epsl.2004.12.005.

Yang, T., Moresi, L., Gurnis, M., Liu, S., Sandiford, D., Williams, S., Capitanio, F.A., 2019. Contrasted East Asia and South America tectonics driven by deep mantle flow. Earth Planet Sci. Lett. 517, 106–116. https://doi.org/10.1016/j.epsl.2019.04.025.

Zindler, A., Hart, S.R., 1986. Chemical geodynamics. Ann. Rev.: Earth Planet Sci. Lett. 14, 493–571. https://doi.org/10.1146/annurev.ea.14.050186.002425.